A double take on early and interacting dark energy from JWST

Journal of Cosmology and Astroparticle Physics
An IOP and SISSA journal

Received: December 27, 2023
Revised: April 25, 2024
Accepted: April 26, 2024
Published: May 20, 2024

A double take on early and interacting dark energy from JWST

Matteo Forconi,[a,b,*] **William Giarè**,[b] **Olga Mena**,[c] **Ruchika**,[a] **Eleonora Di Valentino**,[b] **Alessandro Melchiorri**[a] **and Rafael C. Nunes**[d,e]

[a] *Physics Department and INFN, Università di Roma "La Sapienza", Ple Aldo Moro 2, 00185, Rome, Italy*
[b] *School of Mathematics and Statistics, University of Sheffield, Hounsfield Road, Sheffield S3 7RH, United Kingdom*
[c] *Instituto de Física Corpuscular (CSIC-Universitat de València), E-46980 Paterna, Spain*
[d] *Instituto de Física, Universidade Federal do Rio Grande do Sul, 91501-970 Porto Alegre RS, Brazil*
[e] *Divisão de Astrofísica, Instituto Nacional de Pesquisas Espaciais, Avenida dos Astronautas 1758, São José dos Campos, 12227-010, São Paulo, Brazil*
E-mail: matteo.forconi@roma1.infn.it, w.giare@sheffield.ac.uk, omena@ific.uv.es, ruchika.ruchika@roma1.infn.it, e.divalentino@sheffield.ac.uk, alessandro.melchiorri@roma1.infn.it, rafadcnunes@gmail.com

Abstract: The very first light captured by the James Webb Space Telescope (JWST) revealed a population of galaxies at very high redshifts more massive than expected in the canonical ΛCDM model of structure formation. Barring, among others, a systematic origin of the issue, in this paper, we test alternative cosmological perturbation histories. We argue that models with a larger matter component Ω_m and/or a larger scalar spectral index n_s can substantially improve the fit to JWST measurements. In this regard, phenomenological extensions related to the dark energy sector of the theory are appealing alternatives, with Early Dark Energy emerging as an excellent candidate to explain (at least in part) the unexpected JWST preference for larger stellar mass densities. Conversely, Interacting Dark Energy models, despite producing higher values of matter clustering parameters such as σ_8, are generally disfavored by JWST measurements. This is due to the energy-momentum flow from the dark matter to the dark energy sector, implying a smaller matter energy density. Upcoming observations may either strengthen the evidence or falsify some of these appealing phenomenological alternatives to the simplest ΛCDM picture.

Keywords: high redshift galaxies, dark energy theory, physics of the early universe
ArXiv ePrint: 2312.11074

*Corresponding author.

https://doi.org/10.1088/1475-7516/2024/05/097

JCAP05(2024)097

Contents

1 Introduction

The minimal ΛCDM model of cosmology, described by only six fundamental parameters, has successfully explained a large number of cosmological observations at different scales. Nevertheless, in recent years, several anomalies have emerged, challenging the model across all cosmological epochs.

Currently, the most significant problem — known as the Hubble tension [1–3] — is represented by a mismatch at the level of $\sim 5\sigma$ between the value of the present-day expansion rate of the Universe (H_0) inferred from Planck-2018 CMB observations ($H_0 = 67.4 \pm 0.5\,\mathrm{km\,s^{-1}\,Mpc^{-1}}$ [4]) and the value of the same parameter measured directly from local distance ladder measurements using Type-Ia Supernovae calibrated with Cepheid variable stars ($H_0 = 73 \pm 1\,\mathrm{km\,s^{-1}\,Mpc^{-1}}$ [5]).

Another conundrum, albeit less significant than the Hubble tension, is the so-called S_8 tension. This parameter is closely related to the clustering of matter in the Universe, and its value can be inferred both from the measurements of CMB anisotropies as those from Planck, and — more directly –from the measurements of galaxy lensing made by experiments such as the Dark Energy Survey (DES) [6, 7], and the Kilo-Degree Survey (KiDS) [8, 9]. While Planck data favors larger values of S_8, KiDS and DES seem to prefer lower ones, leading to a well-documented discrepancy ranging between 2 and 3 standard deviations [10].[1]

[1]Very recently the actual disagreement between these experiments has been the subject of careful reevaluation, see, e.g., ref. [11].

JCAP05(2024)097

Yet another emerging anomaly — which is the focal point of this study — pertains to the observations recently released by the James Webb Space Telescope (JWST) of galaxies at very high redshifts (much higher than those commonly explored by large-scale structure galaxy surveys). Interestingly, the preliminary JWST results point towards a population of surprisingly massive galaxy candidates (see e.g. [12–19]) with stellar masses of the order of $M \geq 10^{10.5} M_{\odot}$. In a recent study [20], it was pointed out that the JWST data indicates a higher cumulative stellar mass density in the redshift range $7 < z < 11$ than predicted by the ΛCDM model, questioning one more time the canonical cosmological picture [21–23].

Despite the fact that recent comparisons of photometric and spectroscopic redshifts in overlapping samples of galaxies solidify the evidence for a high space density of bright galaxies at $z \gtrsim 8$ compared to theoretical model predictions [24], the JWST anomalous observations could still hint a lack of accuracy in extracting the intrinsic galaxy properties [25–31]. Other possibilities recently explored include the hypothesis of unusual dense regions due to the currently limited JWST observations (which only cover an area of approximately 38 square arcminutes), as well as the possible presence of unknown systematics in CMB Planck polarization data [32, 33].

Although it is certainly premature to draw any definitive conclusions from these preliminary observations, if neither of the aforementioned possibilities can account for the discrepancies between the JWST results and the theoretical predictions of a baseline ΛCDM cosmology, it may be necessary to consider modifications to the model itself [34–55] or to the galaxy formation process [31, 56–59]. In this work, we take a step forward in this direction by testing alternative models where galaxy evolution could be notably different than in ΛCDM. In particular, we consider extensions related to the dark energy sector of the theory as possible phenomenological alternatives to explain the JWST preliminary findings. We test Early Dark Energy (EDE) and Interacting Dark Energy (IDE) cosmologies as both these extended scenarios, featuring modifications in the growth of structure, might predict a different evolution of perturbations, potentially resulting in the formation of more massive galaxies. We demonstrate that while EDE emerges as an excellent candidate to explain (at least partially) the unexpected JWST preference for larger stellar mass densities, IDE is generally disfavored by JWST measurements, despite yielding higher values of matter clustering parameters σ_8 and S_8.

The structure of the paper is as follows: in section 2 we further elaborate on the reasons why we choose Early Dark Energy and Interacting Dark Energy scenarios and also we define the physics and the basic equations governing the cosmological evolution in these models. In section 3 we describe the main observables considered in this work, namely, the cumulative stellar mass density, the observational data and the likelihoods exploited in the numerical analyses. Section 4 contains our main results. We conclude in section 5.

2 Extended Dark Energy scenarios

Despite the undeniable uncertainties surrounding the preliminary findings from JWST, one might wonder whether these new emerging anomalies could be somehow linked to other well-known longstanding problems in cosmology, such as the Hubble tension. This raises the question of whether they could both originate from a common issue related to our current

JCAP05(2024)097

theoretical understanding of the Universe and, on a broader scale, what kind of beyond-ΛCDM phenomenology (if any) can increase the present-day expansion rate of the Universe while also leading to a higher cumulative stellar mass density at earlier times.

At first glance, this question can even appear misplaced, as these observations are often believed to imply an older universe compared to the ΛCDM predictions. Since the age of the Universe is roughly $\propto 1/H_0$, this would suggest that increasing the Hubble constant could worsen the discrepancy with the observations released by JWST. However, structure formation is influenced by the evolution of primordial density perturbations and the underlying cosmology. Models addressing the Hubble tension often propose modifications at both the background level and in perturbation dynamics. This could allow for comparable or greater structure formation in a younger Universe (various N-body simulations of extension to ΛCDM show such variations, e.g. [60–65]). Furthermore, in beyond-ΛCDM models different correlations among cosmological parameters can shift their fitting values. These effects may significantly impact parameters related to structure formation, such as the matter density Ω_m, and the other matter clustering parameters σ_8 and $S_8 = \sigma_8 \cdot (\Omega_m/0.3)^{1/2}$. These correlations are crucial as they could affect the amplitude and shape of the matter power spectrum.

An exercise certainly useful for understanding which kind of phenomenology could hit two targets with one arrow — increasing H_0 and aligning more closely with JWST — is breaking down the problem into smaller parts. In particular, we focus on the baseline ΛCDM model fixing all parameters to the best-fit values provided by Planck and altering each one individually within a 4-standard-deviation range. Through this analysis, focusing on the JWST likelihood ($\chi^2_{\rm JWST}$), we identify physical adjustments for better consistency with observations. From figure 1 we can derive a quite significant amount of information:

- First and foremost, we observe that the parameter on which $\chi^2_{\rm JWST}$ is most sensitive is the matter density parameter Ω_m. In particular, a larger fraction of matter in the Universe will considerably improve the quality of the fit to JWST observations by facilitating structure formation.[2]

- Secondly, we can clearly note that increasing the amplitude of the primordial perturbations A_s or considering a larger tilt n_s results in a significant reduction in $\chi^2_{\rm JWST}$. This is in line with previous findings documented in ref. [32], where it was argued that relaxing the Planck constraints on polarization, which in turns allows τ to reach considerably higher values [33], can substantially improve the agreement between JWST and CMB data.[3] Similarly, larger n_s can substantially increase the power in the matter power spectrum on small scales, also facilitating more structure to form.

- Finally, concerning H_0, we observe that a straightforward increase in the value of this parameter while simultaneously keeping σ_8 constant worsens the fit to JWST data. This aligns with the argument that, when fixing structure formation parameters, a younger Universe reduces the number of structures that can form. However, the impact of H_0 on $\chi^2_{\rm JWST}$ is relatively small and it proves how the Hubble constant plays only a partial role in a more complex interplay of various parameters.

[2]For similar discussions involving quasars at high redshifts, see, e.g., refs. [66, 67].

[3]Since there exists a well-known degeneracy relation $A_s e^{-2\tau}$, high values of τ can be compensated by higher values of A_s.

JCAP05(2024)097

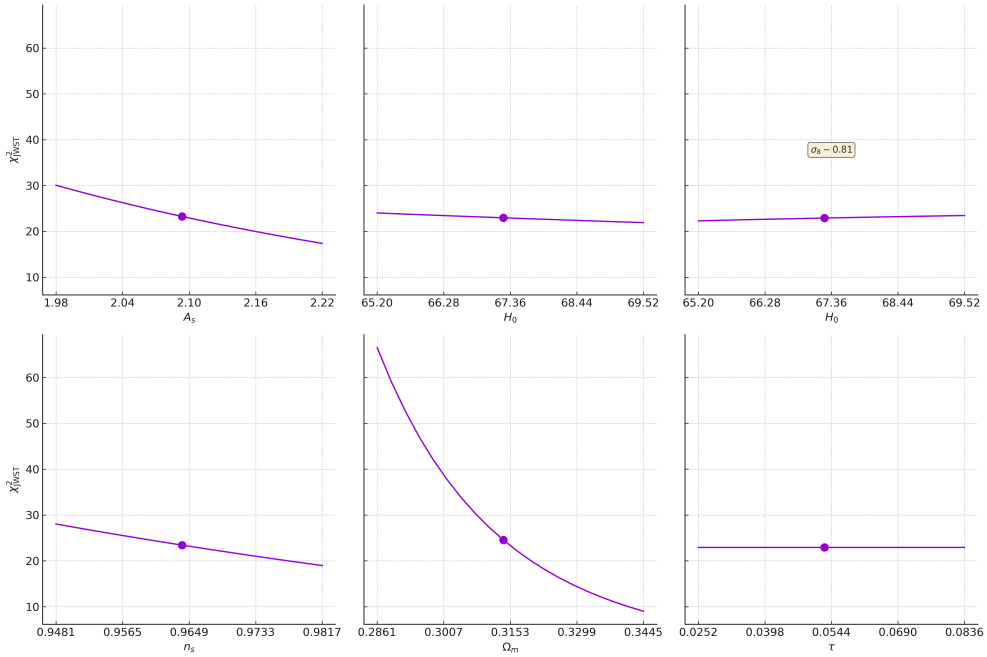

Figure 1. Changes in $\chi^2_{\rm JWST}$ when varying a single parameter while keeping the others fixed to the Planck ΛCDM best-fit values (bold points in the figure): $\Omega_b h^2 = 0.02238$, $\Omega_c h^2 = 0.1201$, $H_0 = 67.32\,\mathrm{km/s/Mpc}$, $n_s = 0.9659$, $A_s \times 10^9 = 2.1$, $\tau = 0.0543$, and $\Omega_m h^2 = 0.143$. In the top panel's third plot, when H_0 is free to vary, σ_8 is kept fixed by rescaling A_s accordingly.

Summarizing these results, from a phenomenological standpoint, an effective model to increase the value of H_0 and improve the agreement with preliminary JWST data should predict a higher spectral index, along with a greater quantity of matter in the Universe and possibly higher values of σ_8 and S_8. On one side, this phenomenology is common in proposals aimed at resolving the Hubble tension by introducing new physical components that act before recombination. For this reason, we explore extensions related to the early Universe and, as a case study, analyze EDE cosmology. On the other hand, larger values of matter clustering parameters σ_8 and S_8 can also be achieved within late-time solutions of the Hubble tension that attempt to modify physics after recombination, influencing the value of H_0 derived from the angular distance from the CMB. Therefore, in the spirit of not leaving anything untried, we also test IDE cosmologies where both the growth of perturbations and the matter clustering are significantly different than in ΛCDM. Below, we summarize the basic aspects of the theoretical models we will be considering.

2.1 Early Dark Energy

Early Dark Energy models are a natural hypothesis of dark energy, see e.g., refs. [68–99]. Deviating from the traditional cosmological constant framework, EDE models account for a non-negligible contribution from dark energy in the early Universe. In addition, these EDE models can be based on a generic dark energy fluids which are inhomogeneous. Their density and pressure vary over time, leading to a non-static equation of state. The phenomenological analyses of these inhomogeneous dark energy models usually require additional dark energy

JCAP05(2024)097

clustering parameters, the dark energy effective sound speed and the dark energy anisotropic stress. The effective sound speed determines the clustering properties of dark energy and consequently it affects the growth of matter density fluctuations. Therefore, in principle, its presence could be revealed in large scale structure observations. The growth of perturbations can also be affected by the anisotropic stress contributions which lead to a damping in the velocity perturbations.

Recently, EDE models have garnered significant attention, particularly due to their potential role in addressing some of the aforementioned cosmological tensions [75, 91, 100]. Our analysis will concentrate on the EDE implementation detailed in [84]. This model proposes that, in the early Universe, a light scalar field deviates from its potential minimum and, constrained by Hubble friction, is functionally similar to a cosmological constant. As soon as, at some particular redshift $z_\star$, the Hubble parameter reduces to be less than the mass of the field, the scalar field rolls down its potential and begins to oscillate about the minimum. To avoid spoiling late-time cosmology, the vacuum energy must redshift away quicker than matter (i.e., faster than a^{-3}), and the field should behave as a subdominant component. A typical set of parameters used in this model is: the fractional contribution to the total energy density of the Universe, $f_{\rm EDE}(z) \equiv \rho_{\rm EDE}(z)/\rho_{\rm tot}(z)$ evaluated at the critical redshift z_c at which it reaches the maximum value, and θ_i, which is the parameter that usually describes the initial field displacement. This particular behavior implies a larger amount of energy-density in the early Universe (just prior to recombination), a reduction of the sound horizon and, consequently, a larger value of the Hubble constant inferred by CMB observations. This is the reason why EDE models have been proposed as a possible solution to the Hubble constant tension.

2.2 Interacting Dark Energy

Interacting Dark Energy models describe a phenomenological scenario where the dark fluids of the Universe interact with each other by allowing a transfer of energy and/or momentum between them, see e.g., refs. [101–155]. Instead, the other components of the Universe (such as radiation and baryons) remain unaffected. The background evolution for dark energy and dark matter is modified, as the continuity equations for the single component present an interaction function Q whose sign governs the energy-momentum flow. A negative value of the interaction rate, $Q < 0$, implies a transfer of energy and/or momentum from pressureless dark matter to dark energy, while the opposite, refers to an energy-momentum flow from the dark energy sector to the dark matter one. In order to solve the background evolution, one would need a specific interaction function Q. Depending on such a function, it can be solved either analytically or numerically, together with the equation for the Hubble rate evolution. In what follows we shall use the well-known interaction rate [101, 102, 156–158]:

$$Q = \xi \mathcal{H} \rho_{\rm de}\,, \tag{2.1}$$

where ξ is a dimensionless coupling parameter. The equation governing the evolution of the density perturbations for the dark sector can be found in [101, 102, 157]. IDE models may suffer from instabilities in the perturbation evolution [101, 156]. Our analysis adheres to

JCAP05(2024)097

the criterion of ref. [102] in terms of the so-called *doom factor*

$$\mathbf{d} = \frac{Q}{3\mathcal{H}(1+w)\rho_{\rm de}}\,, \tag{2.2}$$

which is required to be negative in order to avoid instabilities. Consequently this stability condition for our case is translated into a stable parameter space in which $(1+w)$ and ξ must have opposite sign [102]. Therefore, in the phantom regime in which $(1+w)$ is a negative quantity the dimensionless coupling ξ must be positive. On the other hand, in the quintessence region ξ must be negative. For earlier studies, see [101, 116, 156, 157, 159–166].

We conclude this section with a final remark: even if the interaction scenario considered here is a pure phenomenological model, some studies have shown that using a multi-scalar field action, the coupling function (2.1) can be derived [167]. Therefore, the interaction model of the form given by eq. (2.1) also benefits from a solid theoretical motivation.

3 Methodology

3.1 Theory

To explore the extended dark energy scenarios in relation to the JWST observations, we strictly follow the methodology detailed in ref. [32]. We compute the predicted Cumulative Stellar Mass Density (CSMD hereafter), which is given by

$$\rho_\star(M_\star) \leq \epsilon f_b \int_{z_1}^{z_2}\int_{M_h}^{\infty} \frac{dn}{dM} M dM \frac{dV}{V(z_1,z_2)}\,, \tag{3.1}$$

where we have $M_\star = \epsilon f_b M_{\rm h}$ with $M_\star$ the mass of the galaxy, $M_{\rm h}$ is the halo mass, $f_b = \Omega_b/\Omega_m$ is the cosmic baryon fraction and ϵ is the star formation efficiency of converting baryons into stars. For our analysis, we opt for a conservative approach and fix $\epsilon = 0.2$ following ref. [168]. However, as suggested by ref. [168], in principle star formation efficiency can be a function of the halo mass and further adjustments to star formation physics might be needed for more precise computations [169]. Nonetheless, for the mass scale we are working with, ϵ can only vary smoothly as a function of mass, following a power law. Therefore, given the short mass range we are using in our analyses, this does not change in a significant way our main conclusions. Notice also that we consider the cosmic baryon fraction instead of computing the baryon evolution in different halos [64, 170–175].[4] All these methodological choices and simplifications are widely used in the literature and allow us to present conservative and credible results that, without sacrificing generality, can be directly compared with similar works following the same approach.

Furthermore, $\frac{dn(M,z)}{dM}$ is the comoving number density of the collapsed objects between a mass range from M to $M + \Delta M$ at a certain redshift, given by

$$\frac{dn(M,z)}{dM} = F(\nu)\frac{\rho_m}{M^2}\left|\frac{d\ln\sigma(M,z)}{d\ln M}\right|\,, \tag{3.2}$$

[4]Notice that, with the baryon fraction f_b playing the role of a multiplicative factor in front of the integral (3.1), if f_b increases, the theoretical predictions are proportionally pushed towards the observed data points. Just for reference, fixing f_b as large as $f_b = 0.23$, we find an expected decrease in the χ^2 of about 55%.

JCAP05(2024)097

where ρ_m is the comoving matter density of the Universe, $F(\nu)$ the Sheth-Tormen (ST) Halo mass function [176, 177] and $\sigma(R, z)$ is the variance of linear density field smoothed at a scale R, where we assume a Top-Hat window function. The ST formalism is theoretically motivated in terms of the collapse of halos [178, 179] and has been exhaustively tested by N-body simulations for different dark energy models taking different priors for Ω_m and Ω_Λ [180]. In this study, we assume that the halo mass function of the ST type applies to both theoretical frameworks examined. Nevertheless, analyses of future JWST data may need to consider a more sophisticated fit.

3.2 Observational data

Regarding the JWST observations, given their preliminary nature and the wide research interest they have generated, a multitude of datasets obtained following different methodologies have been released. Consequently, a choice of which dataset to use becomes necessary. In this study, we consider four independent datasets summarized in table 1 and listed below:[5]

- Confirmed CSMD measurements taken from ref. [20]. We find this dataset particularly well-suited for our analysis as it provides explicit constraints on the CSMD that are directly linked to cosmological structure formation. For this dataset, the errors reported in table 1 are assumed to follow a Log Normal distribution. We refer to this dataset as *JWST-CEERS*.

- Five observational CSMD coming from the photometric data of JWST coverage of the UKIDSS Ultra Deep Survey (UDS) and Hubble Ultra Deep Field (HUDF) [182]. The errors for HUDF & UDS displayed in table 1 are conservatively taken as the maximum value, while the stellar masses are set to be equal to $M = 10^8 M_\odot$ as suggested in table 6 of ref. [182]. We refer to this dataset as *JWST-HUDF&UDS*.

- Two values of the observational CSMD coming from optical data in the GLASS-ERS 1324 program [12]. The stellar mass for GLASS datapoints is set to the average between the mass interval reported in table 1 where we refer to this dataset as *JWST-GLASS*.

- JWST FRESCO NIRCam/grism survey [26]. This dataset spans an area of 124 arcmin^2, covering a survey volume of approximately 1.2×10^6 Mpc^3 within the redshift range $z \in [5, 9]$. We refer to it as *JWST-FRESCO*. Taking the *JWST-FRESCO* data at face value (and barring any potential systematic errors), we consider 3 obscured galaxies located within densely dusty regions, with redshifts in the range $5 \lesssim z \lesssim 6$. Referring to figure 3 of ref. [26], we can see that these galaxies show exceptionally extreme properties such as dark matter halo masses of $\log(M_{\rm halo}/M_\odot) = 12.88^{+0.11}_{-0.13}$, $12.68^{+0.23}_{-0.17}$, and $12.54^{+0.17}_{-0.18}$. Notice also that the quantity measured by *JWST-FRESCO* is the cumulative comoving number density of dark matter halos, not the CSMD. For any given model of cosmology, the cumulative comoving number density of dark matter halos can be computed as:

$$n(> M_{\rm halo}) = \int_{z_1}^{z_2} \int_{M_{\rm halo}}^{\infty} \frac{dn}{dM}\, dM, \tag{3.3}$$

[5] Notice that many additional measurements have been released, see, e.g., refs. [26, 181]. In future, these measurements could potentially serve as independent tests of our preliminary findings.

JCAP05(2024)097

z	$\ln(\rho/M_\odot Mpc^{-3})$	$\ln(M/M_\odot)$	Dataset
$7 < z < 8.5$	5.893 ± 0.345	10.030	CEERS [20]
	5.676 ± 0.652	10.75	
$8.5 < z < 10$	5.709 ± 0.386	9.704	
	5.386 ± 0.653	10.408	
$3.5 < z < 4.5$	$7.00^{+0.14}_{-0.16}$	10.48 ± 0.15	HUDF & UDS [182]
$4.5 < z < 5.5$	$6.79^{+0.20}_{-0.28}$	10.45 ± 0.27	
$5.5 < z < 6.5$	$6.67^{+0.21}_{-0.23}$	10.33 ± 0.36	
$6.5 < z < 7.5$	$6.51^{+0.42}_{-0.60}$	10.68 ± 0.79	
$7.5 < z < 8.5$	$5.75^{+0.59}_{-0.1.10}$	[10.70]	
$6.9 < z < 8.5$	5.07 ± 0.52	$7.2 < \ln(M/M_\odot) < 9.3$	GLASS [12]
$3.5 < z < 4.5$	4.52 ± 0.65		
$5 < z < 6$	$\ln(n(> M_{\rm halo})$	$\ln(M_{\rm halo}/M_\odot)$	FRESCO [26]
	$-5.52^{+0.69}_{-0.58}$	$12.88^{+0.11}_{-0.13}$	
		$12.68^{+0.23}_{-0.17}$	
		$12.54^{+0.17}_{-0.18}$	

Table 1. Observational points for JWST for the four different dataset. The values here must be rescaled by the corresponding comoving volume and luminosity distance for the Planck bestfit ΛCDM model.

where the integrand in eq. (3.3) is defined by eq. (3.2). Regarding the error for the FRESCO dataset, we use the approach of Poissonian approximation for small numbers of observed events (the interested reader can refer to our appendix A for more details).

We highlight that in eq. (3.1), $V(z_1, z_2) = \frac{4}{3}\pi \left[R^3(z_2) - R^3(z_1)\right]$ represents the model-dependent comoving volume of the Universe between redshifts z_1 and z_2 (with $R(z)$ being the comoving radius at z). In the values of $\rho^{\rm obs}$ given in table 1, the comoving volume has been derived assuming the best-fit ΛCDM model (`Planck TTTEEE+lowE+lensing` CMB measurements with $h = 0.6732$, $\Omega_m = 0.3158$, $n_s = 0.96605$, $\sigma_8 = 0.8120$, see [20]), making the data points model-dependent, too. As a result, these values need to be appropriately rescaled before interfacing them with the predicted values for dark energy scenarios. That is, they must be corrected by a factor equal to the ratio of the two comoving volumes ($V_\Lambda/V_{\rm DE}$). Similarly, the conversion between luminosity fluxes and distances for the stellar masses has been inferred, again, under the underlying assumption of the best-fit Planck ΛCDM model. A similar rescaling has to be applied, using the squared ratios of the luminosity distances.

JCAP05(2024)097

3.3 Numerical analyses

For our analyses, we perform a Monte Carlo Markov Chain (MCMC) using the publicly available package `Cobaya` [183] and generate theoretical predictions exploiting with a modified version of the software `CLASS` [184, 185] to address the IDE scenario, while, for EDE, the publicly available software `CLASS EDE`,[6] which solves the evolution of the background and of the perturbations in the presence of a scalar field by means of the Klein-Gordon equation. We investigate the posterior distributions of our parameter space through the MCMC sampler developed for CosmoMC [186, 187] and tailored for parameter spaces with a speed hierarchy which also implements the "fast dragging" procedure [188].

The likelihood used for the MCMC analysis are:

- CMB temperature and polarization power spectra from the legacy Planck release [4, 189] with *plik* TTTEEE+low-ℓ+lowE.
- Lensing Planck 2018 likelihood [190], reconstructed from measurements of the power spectrum of the lensing potential.

In the following discussion, we will refer to the combinations of these two datasets simply as CMB. The convergence of the chains obtained with this procedure is assessed using the Gelman-Rubin criterion [191] setting a convergence threshold at $R-1 \lesssim 0.02$.

Once the chains have converged,[7] for each sampled model we calculate the CMSD (or the comoving number density of dark matter halos for the *JWST-FRESCO* mesurements) corresponding to different parameter combinations explored in the MCMC analysis. In particular, we set the cosmology by varying the cosmological parameters $\{\Omega_b, \Omega_c, \theta_s, \tau\}$, the inflationary parameters $\{n_s, A_s\}$ and the extra parameters from EDE $\{f_{\rm EDE}, \log_{10} z_c, \theta_i\}$ and IDE $\{w, \xi\}$. Afterwards, `CLASS` is employed to compute the linear matter power spectrum $P(k, z)$ and subsequently the variance and, taking its derivative, we estimate the Halo mass function, see eq. (3.2). Eventually, through double integration over mass and redshift, eq. (3.1), we arrive at $\rho_\star(M)$. For each point in the MCMC chains obtained within a given cosmological model, we calculate the $\chi^2_{\rm JWST}$ for various datasets listed in table 1. Each dataset corresponds to a distinct $\chi^2_{\rm JWST}$. Specifically, for any given dataset, $\chi^2_{\rm JWST}$ is determined straightforwardly by

$$\chi^2_{\rm JWST} = \sum_i (x_i^{\rm th} - \bar{x}_i)^2/\sigma_i^2, \tag{3.4}$$

where, $\bar{x}_i$ is the observed value, σ_i^2 is its error, $x_i^{\rm th}$ the theoretically predicted quantity and i runs over the number of data points of the specific JWST dataset. We then obtain the updated constraints on the cosmological parameters by re-weighting the MCMC chains, i.e. performing an importance sample, using the package `getdist`.

4 Results

We now discuss the results obtained for the various extended models of Dark Energy considered in this study. To promote better organization of our findings, we divide this section into

[6] https://github.com/mwt5345/class_ede.

[7] The converged chains are taken with 50% of burn-in.

JCAP05(2024)097

Parameter	CMB		JWST-CEERS	CMB+JWST
n_s	0.981	$z_{\rm low}$	0.997	0.981
		$z_{\rm high}$	0.997	0.981
H_0	69.45	$z_{\rm low}$	72.60	69.45
		$z_{\rm high}$	72.60	69.45
σ_8	0.8273	$z_{\rm low}$	0.854	0.8273
		$z_{\rm high}$	0.854	0.8273
τ	0.0575	$z_{\rm low}$	0.0497	0.05753
		$z_{\rm high}$	0.0497	0.05753
Ω_m	0.307	$z_{\rm low}$	0.304	0.307
		$z_{\rm high}$	0.304	0.307
$f_{\rm EDE}$	0.0628	$z_{\rm low}$	0.151	0.0628
		$z_{\rm high}$	0.151	0.0628
χ^2	2772	$z_{\rm low}$	5.75	2782.76 $(2772 + 10.76)$
		$z_{\rm high}$	7.99	2787.34 $(2772 + 15.34)$

Table 2. Results for EDE. We provide the best-fit values of cosmological parameters, namely the combination that minimizes the χ^2 of the fit to the CMB data alone ($\chi^2_{\rm CMB}$), *JWST-CEERS* data alone ($\chi^2_{\rm JWST-CEERS}$), and CMB+JWST-CEERS data ($\chi^2_{\rm CMB+JWST}$).

two minor subsections: in section 4.1 we focus on the results obtained for EDE, while in section 4.2 we present the findings related to IDE.

4.1 Results for Early Dark Energy

We start by examining EDE. For this model, we summarize the best-fit values related to the most relevant parameters in tables 2 to 5, distinguishing the results obtained by considering the four JWST datasets independently.

First and foremost, we examine the best-fit values obtained by exclusively considering CMB measurements from the Planck satellite (indicated as CMB in the table). In this case, the values reported in tables 2 to 5, simply represent the combination of cosmological parameters for which $\chi^2_{\rm CMB}$ $(= 2772)$ acquires its minimum value among those obtained within the MCMC analysis. It is worth noting that we retrieve results widely documented in the literature. In particular, the Planck data, while not showing any substantial preference for a non-vanishing fraction of EDE, produce a best-fit value of $f_{\rm EDE} = 0.06$. This leads to a present-day expansion rate of the Universe $H_0 = 69.45\,{\rm km/s/Mpc}$, which is generally higher than the best-fit value obtained for this parameter within the standard cosmological model. Another point that is worth emphasizing is that for the inflationary spectral index we get a best-fit value $n_s = 0.981$, confirming once more the trend of EDE models in predicting a

JCAP05(2024)097

Parameter	CMB	JWST-HUDF&UDS	CMB+JWST
n_s	0.981	0.997	0.997
H_0	69.45	73.42	73.46
σ_8	0.8273	0.854	0.8498
τ	0.0575	0.0497	0.05179
Ω_m	0.307	0.295	0.2947
$f_{\rm EDE}$	0.0628	0.160	0.159
χ^2	2772	46	2829 $(2783 + 46)$

Table 3. Results for EDE. We provide the best-fit values of cosmological parameters, namely the combination that minimizes the χ^2 of the fit to the CMB data alone ($\chi^2_{\rm CMB}$), *JWST-HUDF&UDS* [182] data alone ($\chi^2_{\rm JWST-HUDFUDS}$), and CMB+*JWST-HUDF&UDS* data ($\chi^2_{\rm CMB+JWST}$).

Parameter	CMB	JWST-GLASS	CMB+JWST
n_s	0.981	0.977	0.978
H_0	69.45	71.30	69.88
σ_8	0.8273	0.8274	0.8267
τ	0.0575	0.03343	0.05103
Ω_m	0.307	0.312	0.312
$f_{\rm EDE}$	0.0628	0.130	0.0853
χ^2	2772	20	2797 $(2774 + 23)$

Table 4. Results for EDE. We provide the best-fit values of cosmological parameters, namely the combination that minimizes the χ^2 of the fit to the CMB data alone ($\chi^2_{\rm CMB}$), *JWST-GLASS* data alone ($\chi^2_{\rm JWST-GLASS}$), and CMB+*JWST-GLASS* data ($\chi^2_{\rm CMB+JWST}$).

Parameter	CMB	JWST-FRESCO	CMB+JWST
n_s	0.981	0.997	0.978
H_0	69.45	72.60	69.88
σ_8	0.8273	0.854	0.8267
τ	0.0575	0.0497	0.0510
Ω_m	0.307	0.304	0.312
$f_{\rm EDE}$	0.0628	0.151	0.0853
$\chi^2_{\rm FRESCO}$	2772	21.42	2804 $(2774 + 30)$

Table 5. Results for EDE. We provide the best-fit values of cosmological parameters, namely the combination that minimizes the χ^2 of the fit to the CMB data alone ($\chi^2_{\rm CMB}$), *JWST-FRESCO* data alone ($\chi^2_{\rm JWST-FRESCO}$), and CMB+*JWST-FRESCO* data ($\chi^2_{\rm CMB+JWST}$).

JCAP05(2024)097

spectrum of primordial perturbations closer to the scale-invariant case than what is observed in ΛCDM and predicted by the most typical inflationary potentials [88, 192–198].[8]

As a second step, following the methodology outlined in the previous section, for each combination of parameters in the MCMC chains (i.e., for each collected model), we calculate the χ^2 against the four different JWST datasets listed in table 1.

We start discussing the results obtained re-weighting the chains in light of $\chi^2_{\rm JWST-CEERS}$ resulting from the *JWST-CEERS* dataset. This dataset has been recently analyzed in many similar studies and allows us for direct comparison with the existing findings in the literature [21, 35]. In this case, we summarize the results in table 2, distinguishing between the low ($z_{\rm low}$) and high ($z_{\rm high}$) redshift bins (also see table 1). Similar to the CMB analysis, we present the specific combination of parameters that minimizes $\chi^2_{\rm JWST-CEERS}$. Furthermore, in figure 2 we provide a triangular plot showing the distribution of sampled models and the correlations among different parameters, together with a color-map representing the value of $\chi^2_{\rm JWST-CEERS}$. For the sake of comparison, in the same figure, we also depict the predictions of ΛCDM. A few intriguing conclusions can be derived from both table 2 and figure 2. Firstly, there are no significant differences between the results obtained for the high and low redshift bins. Secondly, as for the best-fit values of cosmological parameters, we now find a pronounced preference for a non-vanishing fraction of EDE, $f_{\rm EDE} = 0.151$. We also get higher $\sigma_8 = 0.85$ and observe the same trend towards higher values of inflationary spectral index $n_s = 0.997$, now essentially consistent with a Harrison-Zel'dovich spectrum. As pointed out in section 2, this is exactly the kind of phenomenology one needs to increase the agreement with JWST data. Therefore — not surprisingly — the minimum value of $\chi^2_{\rm JWST-CEERS}$ for both the high ($\chi^2_{\rm JWST-CEERS} = 7.99$) and low ($\chi^2_{\rm JWST-CEERS} = 5.75$) redshift bins are significantly better than what we get in ΛCDM (where $\chi^2_{\rm JWST-CEERS} \sim 17$ [32]). This suggests that EDE stands as a valid phenomenological alternative to explain (at least partially) the preliminary measurements released by *JWST-CEERS*. Furthermore, regarding H_0, the *JWST-CEERS* best-fit value reads $H_0 = 72.60\,{\rm km/s/Mpc}$. Therefore, not only within the context of EDE we can improve the agreement between the theoretical predictions of the model and the *JWST-CEERS* data, but to achieve this, we move through the parameter space in the same direction needed to solve the Hubble tension, as well. This is also clearly confirmed by the color pattern in figure 2, underscoring that it is indeed possible to address both issues within the same theoretical framework.

Finally, always in table 2, we present the results inferred by summing up the χ^2 values of CMB and *JWST-CEERS*. We observe that the combination of parameters that minimizes the total $\chi^2_{\rm CMB+JWST}$ is the same as that minimizing the fit to only the Planck data $\chi^2_{\rm CMB}$. At first glance, this implies that the cost of improving the fit to the *JWST-CEERS* data is an overall deterioration in the fit to the CMB. On the other hand, such deterioration is entirely expected, given the strong preference of Planck data for a ΛCDM cosmology and the general disagreement between *JWST-CEERS* data and the latter. As extensively documented in the literature and confirmed by our analysis, individual Planck data do not provide clear evidence in favor of an EDE cosmology. In any case, the best-fit parameters

[8] For other discussions surrounding the value of this parameter and the agreement among the results of different CMB probes, see, e.g., refs. [199–207].

JCAP05(2024)097

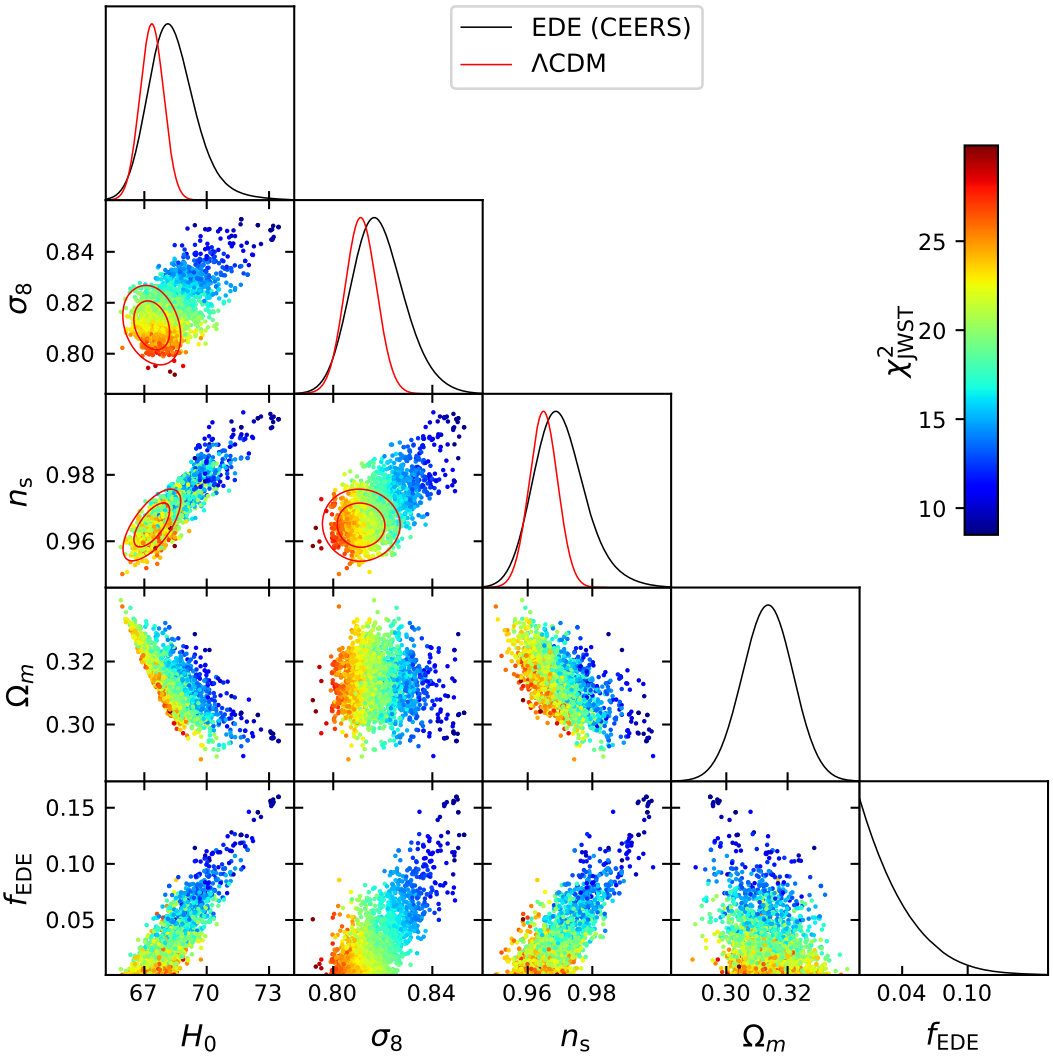

Figure 2. Triangular plot showing the distribution of points and the correlations among the most relevant parameters of EDE. The color map refers to the value of $\chi^2_{\rm JWST}$ so that the color pattern in the figure represents the direction towards which one needs to move in the parameter space to improve the fit to JWST data.

suggest an inclination towards a model where the fraction of EDE remains modest and well below $f_{\rm EDE} \lesssim 0.1$. In contrast, reconciling *JWST-CEERS* with an EDE cosmology would require an EDE fraction $f_{\rm EDE} \gtrsim 0.1$. Forcing such an EDE fraction into the model would source significant effects in the CMB spectra that can only be partially compensated by the observed shift in the fitting values of other cosmological parameters. Just to provide an illustrative example, the increase in the expansion rate of the Universe before recombination due to a substantial EDE component leads to a significant reduction in the value of the sound horizon at the combination, forcing the value of H_0 in the direction of SH0ES, which is certainly not the direction favored by CMB data. Additionally, since EDE does not alter the physics of post-recombination, a higher H_0 implies a lower angular diameter distance from the CMB, D_A. In turn, this leads to a shift in the wavenumber associated with the

JCAP05(2024)097

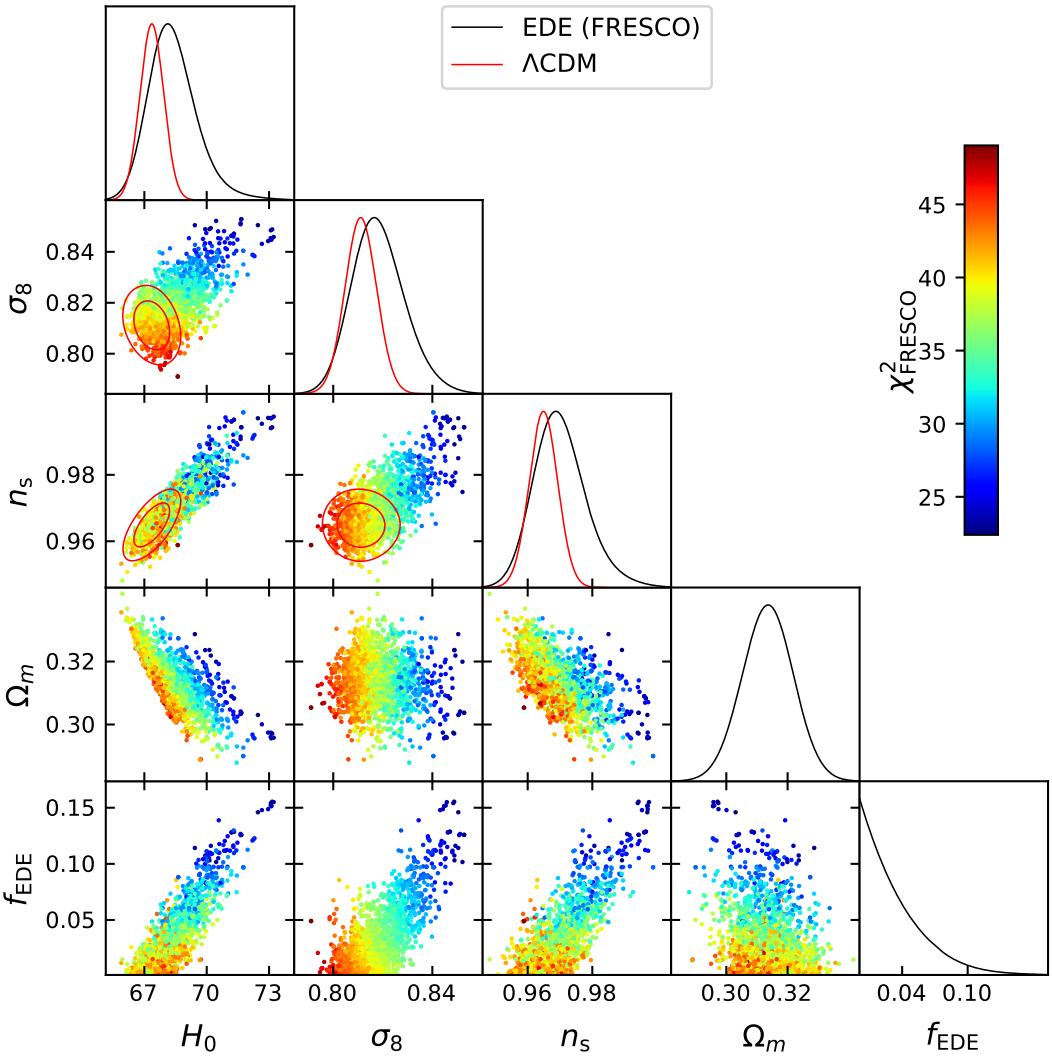

Figure 3. Triangular plot showing the distribution of points and the correlations among the most relevant parameters of EDE. The color map refers to the value of $\chi^2_{\rm FRESCO}$ so that the color pattern in the figure represents the direction towards which one needs to move in the parameter space to improve the fit to JWST FRESCO data.

damping tail k_D, as these two parameters are related by the relationship $\ell_D \sim k_D D_A$, where the multipole ℓ_D is also fixed by CMB measurements. In an attempt to maintain a good fit to the damping scale, the value of n_s is shifted towards a scale-invariant primordial spectrum (i.e., $n_s \to 1$) which certainly improves the agreement between *JWST-CEERS* and EDE but is again highly disfavored by Planck (by over 8σ in ΛCDM). Overall, all these effects and shifts in the fitting values of cosmological parameters seem to favor *JWST-CEERS* observations. However, although they partially compensate for each other, they still remain somewhat disfavored based solely on CMB data, leading to a deterioration in the fit.

When analyzing the other JWST datasets listed in table 1, all the conclusions we have drawn so far remain mostly true. For instance, by comparing the results obtained for *JWST-CEERS* in figure 2 with those obtained for *JWST-FRESCO* in figure 3, at first glance, we

JCAP05(2024)097

can spot the very same color patterns, indicating that a non-vanishing fraction of EDE could, in principle, help to reduce $\chi^2_{\rm FRESCO}$ while also yielding higher values of H_0. However, paying closer attention to the colorbar scale, we observe that as we approach the limit $f_{\rm EDE} \to 0$ moving towards the ΛCDM cosmology, we get $\chi^2_{\rm JWST-FRESCO} \sim 50$ for 3 data points. This value can be reduced all the way down to $\min(\chi^2_{\rm JWST-FRESCO}) \sim 21.42$ when $f_{\rm EDE} \sim 0.15$ and $H_0 \sim 73\,{\rm km/s/Mpc}$, as seen in table 5. On one hand, this lends weight to the idea that EDE could potentially pave the way to partially explaining more massive galaxies and higher values of H_0. On the other hand, it is important to note a nearly threefold increase in $\chi^2_{\rm JWST-FRESCO}$ compared to the results obtained for *JWST-CEERS*. Taking the large χ^2 at face value, we must draw the conclusion that the *JWST-FRESCO* dataset remains in strong disagreement with the theoretical predictions of the standard cosmological model and — to a lesser extent — with EDE as well.

Looking at the χ^2 of *JWST-GLASS* and *JWST-HUD&UDS*, a similar conclusion can be drawn. As a result, we conclude that while EDE represents a phenomenological possibility to partially address the JWST data, it falls short of being exhaustive in fully addressing issues, leaving the quest for a more comprehensive solution wide open.

Having that said, it is worth keeping in mind some caveats surrounding the joint analyses. For instance, the total $\chi^2_{\rm CMB+JWST}$ is obtained by considering the sum of χ^2 for each sampled model in the MCMC chains *afterward* and not through a joint analysis of the two experiments from the outset. Additionally, only CMB data are taken into account in the MCMC analysis, which we know do not favor high values of $f_{\rm EDE}$ and H_0. Considering other datasets, such as the measurements of the expansion rate provided by the SH0ES collaboration, could lead to significantly different results in terms of the χ^2 analysis, as typically pointed out by the EDE community (see, e.g., the discussion on page 25 of ref. [75]). Hence, a full joint likelihood analysis of all these datasets (which is beyond the aim of this work) is needed before deriving any definitive conclusions on this matter.

4.2 Results for Interacting Dark Energy

We now move to the study of IDE. In this case, we consider three different models: the usual IDE cosmology with a fixed dark energy equation of state $w \simeq -1$, and wIDE models where the equation of state parameter w is free to vary, although limited either in quintessence ($w > -1$) or phantom ($w < -1$) regime. For the sake of simplicity, in this subsection, we present *only* the results obtained from *JWST-CEERS*. Several well-motivated reasons underpin this decision. Firstly, no significant differences emerged in the results for EDE when analyzing the four different JWST datasets listed in table 1. Overall, all these observations converge on anomalous galaxies that are more massive than predicted by the standard cosmological model. Therefore, no significant disparities are anticipated when analyzing the same four datasets across the various IDE models proposed in this section. Yet another motivation involves noting that addressing these JWST anomalous observations requires a somewhat clear beyond-ΛCDM phenomenology that none of the three IDE models proposed here can offer. To streamline the analysis and emphasize this point, we focus on *JWST-CEERS*, which will provide the phenomenological guidelines applicable directly to all datasets not explicitly mentioned, without exception.

JCAP05(2024)097

Parameter	CMB		JWST-CEERS	CMB+JWST
n_s	0.971	$z_{\rm low}$	0.968	0.963
		$z_{\rm high}$	0.968	0.961
H_0	70.98	$z_{\rm low}$	67.43	68.27
		$z_{\rm high}$	67.43	66.69
σ_8	1.09	$z_{\rm low}$	0.878	0.89
		$z_{\rm high}$	0.878	0.85
τ	0.057	$z_{\rm low}$	0.0609	0.057
		$z_{\rm high}$	0.0609	0.051
Ω_m	0.214	$z_{\rm low}$	0.301	0.315
		$z_{\rm high}$	0.301	0.285
ξ	-0.28	$z_{\rm low}$	-0.0734	-0.098
		$z_{\rm high}$	-0.073	-0.053
χ^2	2781	$z_{\rm low}$	12.50	2800.79 (2785 + 15.79)
		$z_{\rm high}$	18.22	2809.29 (2788 + 21.29)

Table 6. Results for IDE, with the dark energy equation of state fixed to $w \simeq -1$. We provide the best-fit values of cosmological parameters, namely the combination that minimizes the χ^2 of the fit to the CMB data alone ($\chi^2_{\rm CMB}$), *JWST-CEERS* data alone ($\chi^2_{\rm JWST-CEERS}$), and CMB+JWST data ($\chi^2_{\rm CMB+JWST}$).

Table 6 displays the results for the IDE model with a fixed dark energy equation of state. Similar to EDE, we consider three different combinations of data: CMB, *JWST-CEERS*, and CMB+*JWST-CEERS*. In the table, we always show the combination of parameters that minimizes the χ^2 for these three datasets. When focusing solely on the Planck CMB data, we note that the best-fit value for the parameter encapsulating new physics — i.e., the coupling ξ — reads $\xi = -0.28$. This suggests a quite significant transfer of energy-momentum from the dark matter sector to the dark energy sector. As widely documented in the literature, such a transfer of energy-momentum leads to a higher present-day expansion rate of the Universe, whose best-fit value reads $H_0 = 70.98\,{\rm km/s/Mpc}$ (significantly higher than in the standard cosmological model). Furthermore, while we do not observe significant differences in the value of the spectral index, we notice a tendency toward higher values of $\sigma_8 = 1.09$. This makes the model potentially interesting for JWST. Nevertheless, the results we obtain from *JWST-CEERS* data seem to indicate precisely the opposite. In contrast to the CMB fit (which prefers $\xi < 0$), when considering only the *JWST-CEERS* likelihood, the coupling parameter ξ tends towards $\xi \to 0$. Consequently, we lose any ability to increase the present-day expansion rate, getting a best fit value $H_0 = 67.43\,{\rm km/s/Mpc}$. Figure 4 further reinforces our conclusions: it is not n_s but Ω_m that now assumes a critical role. When moving in the direction $\xi < 0$, the matter density undergoes a significant decrease due to

JCAP05(2024)097

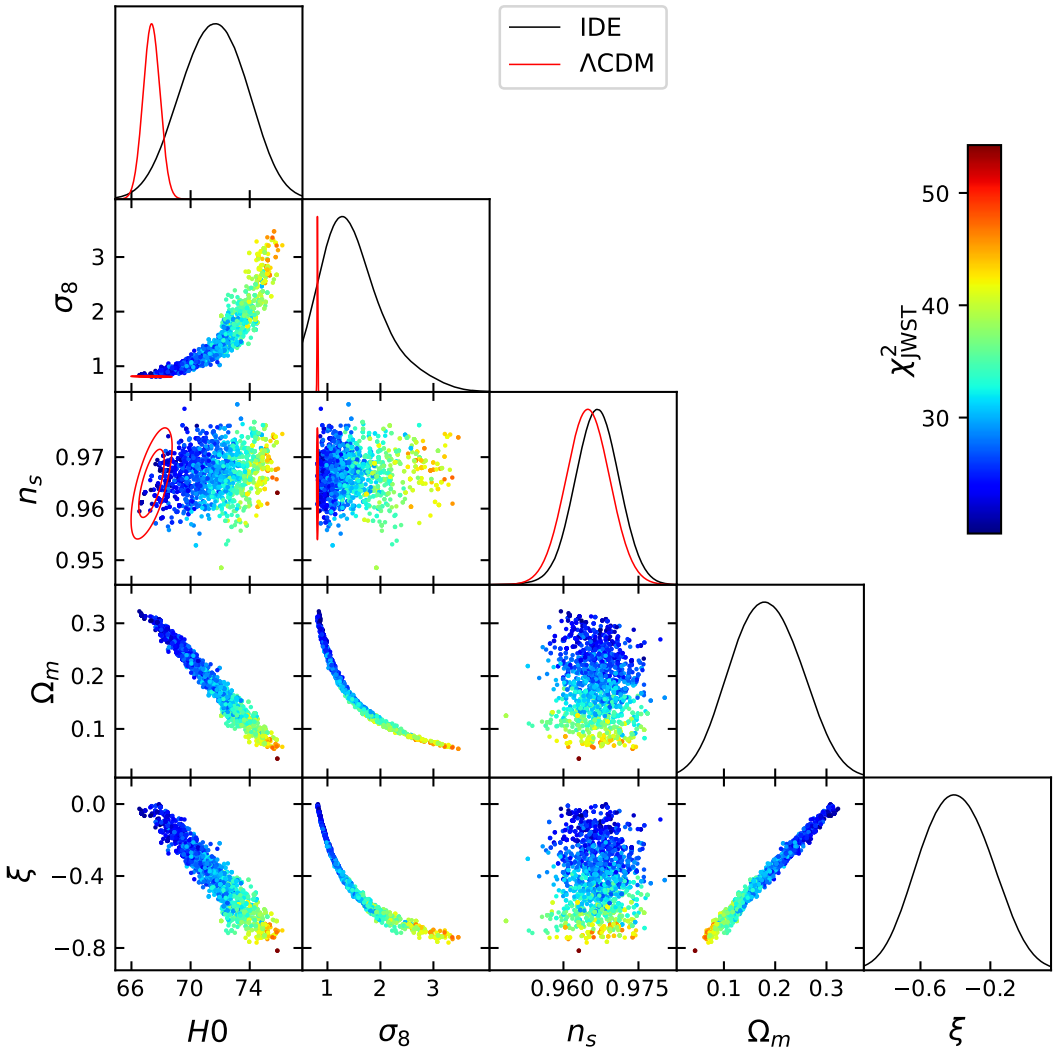

Figure 4. Triangular plot showing the distribution of points and the correlations among the most relevant parameters of IDE, when w is fixed to $w \simeq -1$. The color map refers to the value of $\chi^2_{\rm JWST}$ so that the color pattern in the figure represents the direction towards which one needs to move in the parameter space to improve the fit to JWST data.

the energy transfer from dark matter to dark energy. This leads to a substantial increase in the value of σ_8 to compensate for the reduced Ω_m. However, as illustrated by the color pattern in figure 4, in order to minimize $\chi^2_{\rm JWST-CEERS}$, it becomes necessary to revert to the ΛCDM framework by preventing such energy transfer, essentially moving towards $\xi \to 0$. This behaviour is further supported by comparing the best-fit values of Ω_m (σ_8) for CMB and JWST: while in the former case $\Omega_m = 0.214$ ($\sigma_8 = 1.09$), for *JWST-CEERS*, we get back to more typical values $\Omega_m = 0.301$ ($\sigma_8 = 0.878$). Consequently, this model fails to provide a satisfactory fit to the *JWST-CEERS* observations.

The best-fit values of cosmological parameters for the wIDE model with $w > -1$ (i.e., confined to the quintessence regime) are displayed in table 7. Qualitatively, these results mirror those previously obtained for $w = -1$. There are no differences between the high

JCAP05(2024)097

Parameter	CMB		JWST-CEERS	CMB+JWST
n_s	0.9615	$z_{\rm low}$	0.967	0.9614
		$z_{\rm high}$	0.967	0.9614
H_0	67.35	$z_{\rm low}$	65.44	64.92
		$z_{\rm high}$	65.44	64.92
σ_8	0.9342	$z_{\rm low}$	0.839	0.871
		$z_{\rm high}$	0.839	0.871
τ	0.05742	$z_{\rm low}$	0.0686	0.055
		$z_{\rm high}$	0.0686	0.055
Ω_m	0.274	$z_{\rm low}$	0.326	0.314
		$z_{\rm high}$	0.326	0.314
ξ	-0.1743	$z_{\rm low}$	-0.045	-0.115
		$z_{\rm high}$	-0.045	-0.115
w	-0.9483	$z_{\rm low}$	-0.923	-0.90
		$z_{\rm high}$	-0.923	-0.90
χ^2	2774	$z_{\rm low}$	11.94	2790.89 $(2776 + 14.89)$
		$z_{\rm high}$	17.5	2797.63 $(2778 + 21.63)$

Table 7. Results for wIDE, with $w > -1$ free to vary in the quintessence regime. We provide the best-fit values of cosmological parameters, namely the combination that minimizes the χ^2 of the fit to the CMB data alone ($\chi^2_{\rm CMB}$), *JWST-CEERS* data alone ($\chi^2_{\rm JWST-CEERS}$), and CMB+JWST data ($\chi^2_{\rm CMB+JWST}$).

and low redshift bins, and there is no preference for $\xi \neq 0$ from *JWST-CEERS* data. The behaviors of the parameters depicted in figure 5 clearly indicate that introducing a coupling while leaving w free to vary does not improve the fit to *JWST-CEERS* observations. Once more, the reason behind this phenomenon is the decrease in matter density resulting from the energy flow within the interacting model.

The situation becomes somewhat more intricate when we turn to the case where the dark energy equation of state is confined to the phantom regime $w < -1$. In this case, the best-fit values of parameters are summarized in table 8 for the usual combinations of datasets. When considering only the best-fit values from the CMB, we find the well-documented Planck preference for a phantom equation of state [208, 209], with the best-fit value reading $w = -2.04$. Given the well-known degeneracy between the effects produced by a phantom w and increasing the present-day expansion rate of the Universe, interacting phantom models can provide a much larger value of H_0 [147] and, in fact, we obtain a best-fit value $H_0 = 103.8\,{\rm km/s/Mpc}$. This essentially indicates that, without including datasets at lower redshifts, breaking this line of degeneracy proves challenging and values

JCAP05(2024)097

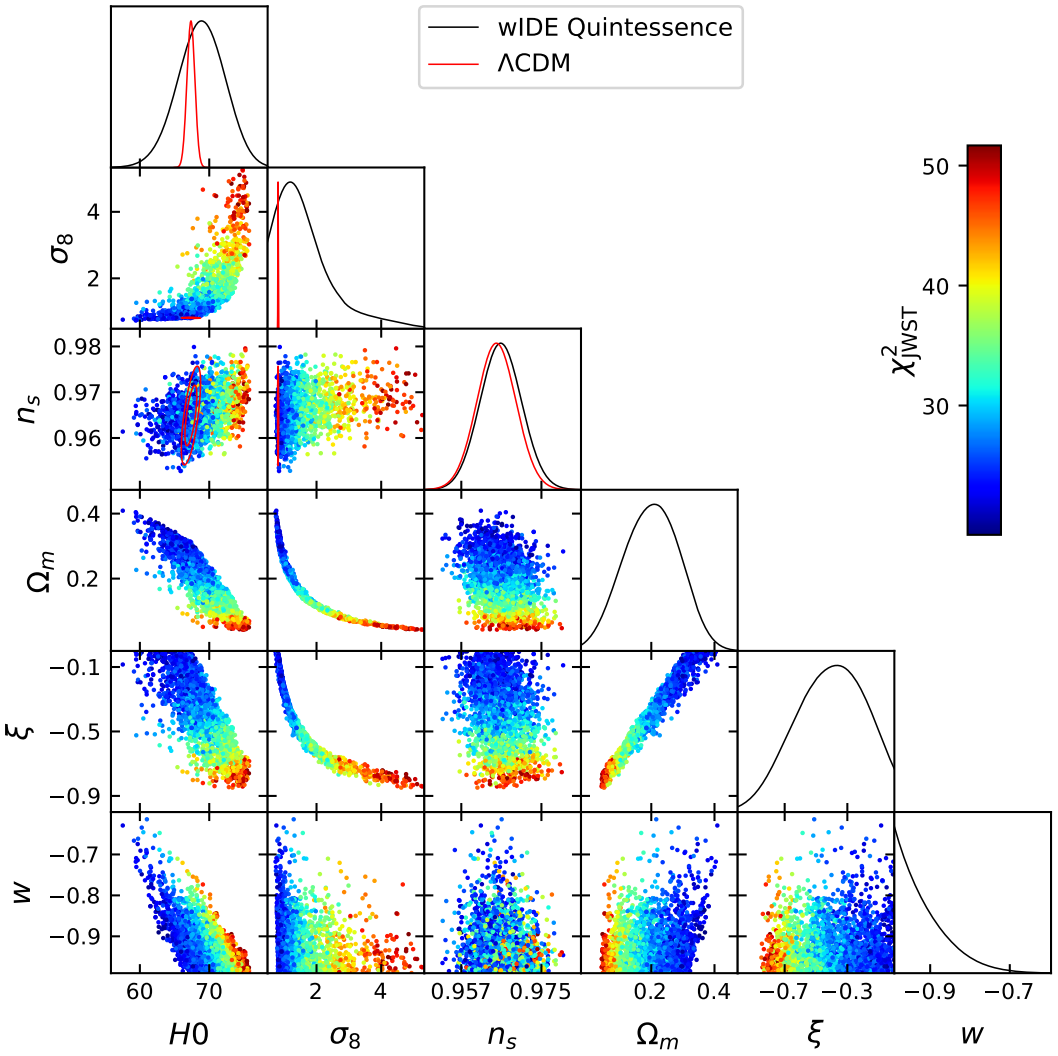

Figure 5. Triangular plot showing the distribution of points and the correlations among the most relevant parameters of wIDE, when w is free to vary in the quintessence region $w > -1$. The color map refers to the value of $\chi^2_{\rm JWST}$ so that the color pattern in the figure represents the direction towards which one needs to move in the parameter space to improve the fit to JWST data.

of H_0 in line with those measured by SH0ES collaboration can always be reintroduced by considering a sufficiently phantom dark energy component. In addition, due to a combination of correlations among different parameters such as H_0, w, and Ω_m, we observe that for the latter parameter, the best-fit value reads $\Omega_m = 0.139$ and is compensated by a substantial increase in $\sigma_8 = 1.026$. In light of these effects on parameters governing the matter clustering in the Universe, the question of whether (and to what extent) a phantom wIDE model could effectively contribute to explaining the anomalies observed in JWST remains a topic of debate. Looking at the brighter side, when we consider the fit to *JWST-CEERS* data, we observed that both for the high ($\chi^2_{\rm JWST-CEERS} = 16.3$) and low ($\chi^2_{\rm JWST-CEERS} = 10.8$) redshift bins, $\chi^2_{\rm JWST-CEERS}$ slightly improves compared to the standard cosmological model. Furthermore, the *JWST-CEERS* data seem to point toward a non-zero coupling $\xi \sim 0.2 - 0.3$,

JCAP05(2024)097

Parameter	CMB		JWST-CEERS	CMB+JWST
n_s	0.9663	$z_{\rm low}$	0.963	0.969
		$z_{\rm high}$	0.967	0.969
H_0	103.8	$z_{\rm low}$	67.10	75.62
		$z_{\rm high}$	73.88	75.62
σ_8	1.026	$z_{\rm low}$	0.685	0.760
		$z_{\rm high}$	0.739	0.760
τ	0.05087	$z_{\rm low}$	0.0612	0.0617
		$z_{\rm high}$	0.0644	0.0617
Ω_m	0.139	$z_{\rm low}$	0.396	0.292
		$z_{\rm high}$	0.319	0.292
ξ	0.05235	$z_{\rm low}$	0.374	0.229
		$z_{\rm high}$	0.299	0.229
w	-2.0436	$z_{\rm low}$	-1.149	-1.33
		$z_{\rm high}$	-1.33	-1.33
χ^2	2767	$z_{\rm low}$	10.8	2783.90 $(2771 + 12.90)$
		$z_{\rm high}$	16.3	2790.15 $(2771 + 19.15)$

Table 8. Results for wIDE with $w < -1$ free to vary in the phantom regime. We provide the best-fit values of cosmological parameters, namely the combination that minimizes the χ^2 of the fit to the CMB data alone ($\chi^2_{\rm CMB}$), *JWST-CEERS* data alone ($\chi^2_{\rm JWST-CEERS}$), and CMB+JWST data ($\chi^2_{\rm CMB+JWST}$).

which is substantially higher than that preferred by the Planck data (whose best-fit value is $\xi \simeq 0.05$). The reason underlying this preference is that to ensure the stability of the perturbations, ξ is now required to be positive. This results in a shift of the energy flow from the dark energy sector to the dark matter one. Consequently, increasing the value of the coupling means injecting more power into the matter sector, facilitating structure formation, and improving the *JWST-CEERS* fit. However, looking at figure 6 — where, as usual, we plot the correlations among different parameters together with a color-map representing the value of $\chi^2_{\rm JWST-CEERS}$ — it becomes really difficult to identify a color pattern representing the direction in which we need to move in the parameter space to improve the fit to *JWST-CEERS* data. Despite this, with a good degree of imagination, we can speculate that by moving towards larger values of the coupling $\xi \to 0.4$ (corresponding to other values of $\Omega_m \to 0.4$), the value of $\chi^2_{\rm JWST-CEERS}$ seems to undergo a general improvement for the highlighted reasons, and its value becomes as good as the ΛCDM one. Interestingly, looking again at figure 6, we note that the value of the Hubble rate corresponding to such a coupling is $H_0 \sim 70\,{\rm km/s/Mpc}$, i.e., close to the result provided by SH0ES collaboration.

JCAP05(2024)097

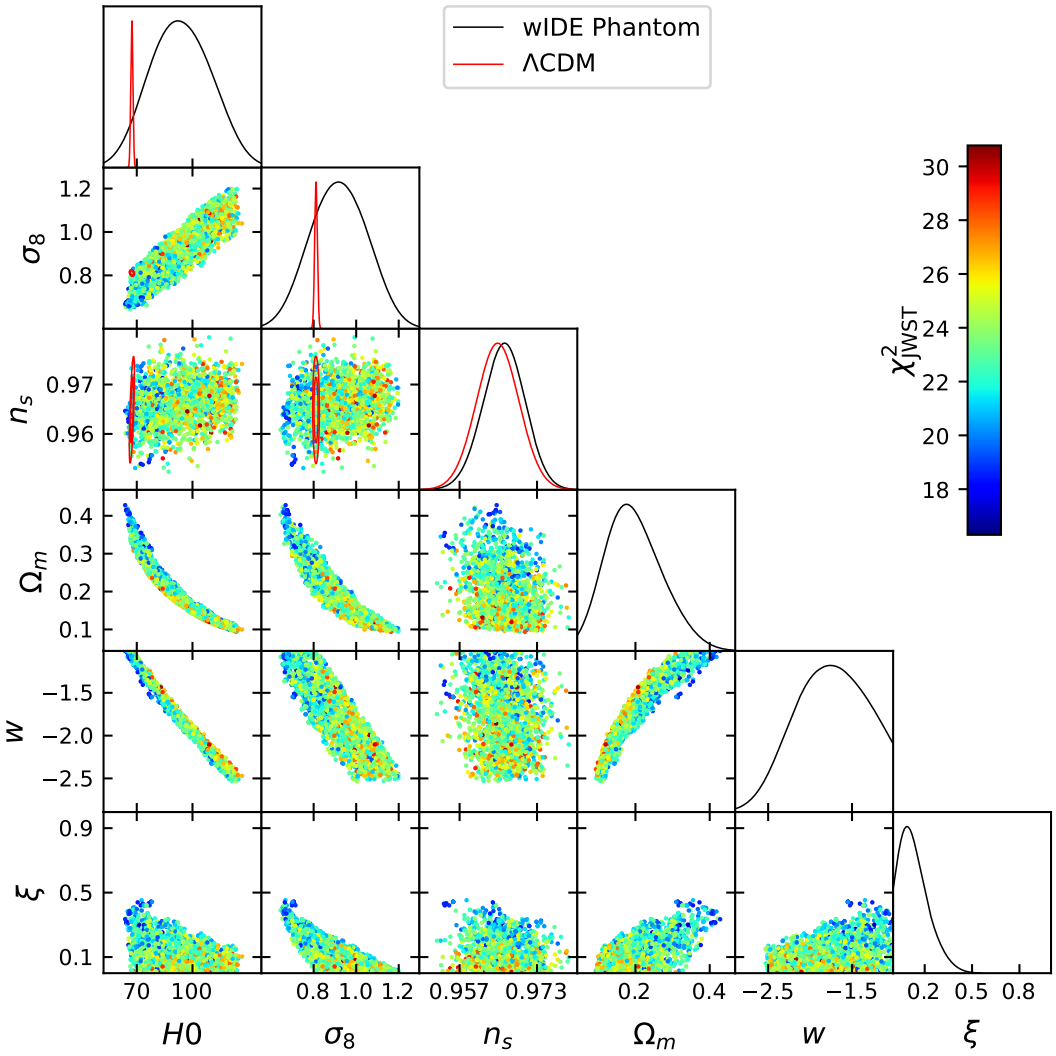

Figure 6. Triangular plot showing the distribution of points and the correlations among the most relevant parameters of wIDE, when w is free to vary in the phantom region $w < -1$. The color map refers to the value of $\chi^2_{\rm JWST}$ so that the color pattern in the figure represents the direction towards which one needs to move in the parameter space to improve the fit to JWST data.

Therefore, in the context of IDE cosmology, the only potential scenario in which we can simultaneously slightly improve the agreement between the model predictions and JWST data while obtaining values of H_0 in line with local distance ladder measurements seems to involve considering a phantom component of the equation of state of dark energy. That being said, the ability of this model to address these two issues remains somewhat limited, above all when compared to the competing EDE solutions discussed in the previous section.

5 Discussion and conclusions

Cosmological data have entered an era of high precision. Advanced telescopes with higher sensitivity are unveiling measurements at previously uncharted cosmological scales and epochs. However, this is a double-edged sword: while high-precision parameter extraction became

JCAP05(2024)097

achievable, a range of unexplained anomalies emerged, some of them growing in significance rather than diluting as the error bars decreased.

The most recent anomaly involves the JWST observations of a population of very high-mass galaxies at previously unexplored redshifts of $z \sim 7 - 10$. This suggests a higher cumulative stellar mass density in the redshift range $7 < z < 11$ than predicted by the standard ΛCDM model of cosmology. Assuming no systematic issue behind these preliminary findings, one might wonder whether these emerging anomalies could be somehow connected to other long-standing cosmological puzzles, such as the Hubble tension. All these issues might hint at a shared limitation in our current comprehension of the Universe, motivating the need to consider alternative theoretical scenarios.

In this paper, taking the four independent JWST datasets at face value, we first explore the correlation between the JWST likelihood and the fundamental six-ΛCDM parameters. We argue that, from a phenomenological standpoint, models with a larger matter component Ω_m, a higher amplitude of primordial inflationary fluctuations A_s and a bigger scalar spectral index n_s are able to predict larger cumulative stellar mass densities, thus providing a better fit to JWST data. As a next step, we notice that part of this phenomenology is very common in models featuring new physics in the dark energy sector (both at early and late times) that have been recently proposed as possible solutions to the Hubble tension. In such models the behavior of the dark energy fluid can also influence the growth of structure, potentially leading to the formation of more massive galaxies able to account for the preliminary JWST measurements. Inspired by this idea, we explore whether in the context of Early Dark Energy or Interacting Dark Energy, the JWST findings could be explained, or at least, if within these scenarios, the fit to JWST observations is improved with respect to the one in the minimal ΛCDM framework.

We find that EDE, which leads to an increased Ω_m and n_s concurrent with a rising EDE fraction $f_{\rm EDE}$, constitutes an excellent candidate. Not only we can improve the agreement between the theoretical predictions of the model and the JWST data (i.e., the minimum value of $\chi^2_{\rm JWST}$ obtained for both the high and low redshift bins is significantly better than what we get in ΛCDM), but to achieve this, we move through the parameter space in the same direction needed to solve the Hubble tension. This underscores that it is indeed possible to address both issues within the same theoretical framework.

Conversely, wIDE models featuring a dark energy equation of state $w \geq -1$ are generally disfavored from JWST, despite yielding higher values of matter clustering parameter σ_8. This is due to the energy flow from the dark matter sector to the dark energy one, implying a smaller Ω_m. On the other hand, when the equation of state is confined to the phantom regime $w < -1$, the situation becomes somewhat more intricate. Whether, and to what extent, a phantom wIDE model could effectively contribute to explaining the anomalies observed in JWST findings remains an open question. The energy-momentum dynamics and parameter degeneracies can lead to a significant increase in the matter component, which in turn can slightly improve the agreement between the model predictions and the JWST data while also yielding values of H_0 in line with local distance ladder measurements. However, the ability of this model to address these two issues simultaneously remains limited compared to EDE.

We conclude by pointing out that other studies have recently investigated dark energy and dark matter alternatives to reconcile the JWST anomalies. Just to mention a few

JCAP05(2024)097

appealing possibilities, in ref. [35] it was argued that adjusting the dark energy sector to accommodate a dynamic equation of state can be compatible with existing observations. However, this would require considering somewhat exotic dynamical dark energy models that necessitate specific configurations of dark energy parameters. Always in relation to the dark energy sector of the cosmological model, in refs. [34, 47], it was argued that an evolving DE component with positive energy density on top of a negative cosmological constant can be consistent with JWST observations. Other different yet interesting possibilities explored to approach the structure formation dilemma involve considering extensions related to particle physics, such as Fuzzy Dark Matter models consisting of ultra-light axions [37] or Warm Dark Matter [39, 40]. Axion models have the potential to mitigate the formation of smaller structures, aligning JWST's stellar mass density data with the CMB optical depth near $z \approx 8$. Instead, Warm Dark Matter models introduce a structural formation delay, predicting fewer low-mass systems at higher redshifts. However, it is worth noting that up until now, observations do not conflict with predictions from either cold dark matter or Warm Dark Matter theories for particles heavier than 2 keV [39]. Finally, another category of solutions competitive with those examined in this study frequently proposes new physics in the gravitational sector. For instance, if long-range attractive forces stronger than gravity are realized in nature, the formation of cosmic halos could begin during the radiation-dominated era, providing a possible explanation for the excess of heavy galaxies observed by JWST.

Future JWST data will either reinforce or diminish the need for exploring physics beyond the established ΛCDM scenario.

Acknowledgments

MF, R and AM thank TASP, iniziativa specifica INFN for financial support. EDV is supported by a Royal Society Dorothy Hodgkin Research Fellowship. The work of AM was supported by the research grant number 2022E2J4RK "PANTHEON: Perspectives in Astroparticle and Neutrino THEory with Old and New messengers" under the program PRIN 2022 funded by the Italian Ministero dell'Università e della Ricerca (MUR). RCN thanks the financial support from the Conselho Nacional de Desenvolvimento Científico e Tecnologico (CNPq, National Council for Scientific and Technological Development) under the project No. 304306/2022-3, and the Fundação de Amparo à pesquisa do Estado do RS (FAPERGS, Research Support Foundation of the State of RS) for partial financial support under the project No. 23/2551-0000848-3. This article is based upon work from COST Action CA21136 Addressing observational tensions in cosmology with systematics and fundamental physics (CosmoVerse) supported by COST (European Cooperation in Science and Technology). We acknowledge IT Services at The University of Sheffield for the provision of services for High Performance Computing. The work of OM is supported by the Spanish grant PID2020-113644GB-I00 and by the European Union's Framework Program for Research and Innovation Horizon 2020 (2014–2020) under grant H2020-MSCA-ITN-2019/860881-HIDDeN and SE project ASYMMETRY (HORIZON-MSCA-2021-SE-01/101086085-ASYMMETRY) and well as by the Generalitat Valenciana grant CIPROM/2022/69.

JCAP05(2024)097

A JWST-FRESCO survey uncertainty approximation

In this appendix, we provide additional details about the methodology we used to derive the uncertainty on the cumulative comoving number density of dark matter halos $\Delta \log n$ for *JWST-FRESCO*. We use the same statistical methodology adopted in refs. [35, 47] and introduced in refs. [210, 211]. At its core, the methodology relies on approximations to the exact Poissonian confidence limits for small numbers of observed events (that in our case is 3). More quantitatively, we approximate the true Poissonian upper limit, by means of eq. (4) of ref. [211], that, for 3 events, reads

$$\Delta \log n_{\rm upper} = 4 \left[\frac{35}{36} + \frac{S}{6} + 4^{c(S)} b(S) \right]^3 , \tag{A.1}$$

where we fix $S \simeq 1.645$ which corresponds to choosing a 95%CL interval uncertainty,[9] see also the third column of table 3 in ref. [210]. Notice also that, once S is fixed, $c(S)$ and $b(S)$ are numerical coefficients that can be easily calculated by using eqs. (6)–(7) in ref. [211]. Similarly, adopting eq. (11) of ref. [211], we estimate the lower limit on the error bar as:

$$\Delta \log n_{\rm lower} = 4 \left[\frac{26}{27} + \frac{S}{3\sqrt{3}} + 3^{\gamma(S)} \beta(S) + \delta(S) \sin\left(\frac{10\pi}{13} \right) \right]^3 \tag{A.2}$$

where, as usual, $S \simeq 1.645$ and $\beta(S)$, $\gamma(S)$ and $\delta(S)$ are given by eqs. (9), (10) and (12) of ref. [211], respectively. We stress that this statistical methodology, while accurate, necessarily introduces an additional layer of approximation. For this reason, we remain conservative proving the uncertainties on $\log n(> M_{\rm halo})$ at 95% CL (corresponding to fixing $S \simeq 1.645$).

References

[1] L. Verde, T. Treu and A.G. Riess, *Tensions between the Early and the Late Universe*, *Nature Astron.* **3** (2019) 891 [arXiv:1907.10625] [INSPIRE].

[2] E. Di Valentino et al., *Snowmass2021 — Letter of interest cosmology intertwined II: The hubble constant tension*, *Astropart. Phys.* **131** (2021) 102605 [arXiv:2008.11284] [INSPIRE].

[3] E. Di Valentino et al., *In the realm of the Hubble tension — a review of solutions*, *Class. Quant. Grav.* **38** (2021) 153001 [arXiv:2103.01183] [INSPIRE].

[4] PLANCK collaboration, *Planck 2018 results. VI. Cosmological parameters*, *Astron. Astrophys.* **641** (2020) A6 [*Erratum ibid.* **652** (2021) C4] [arXiv:1807.06209] [INSPIRE].

[5] A.G. Riess et al., *A comprehensive Measurement of the Local Value of the Hubble Constant with 1 km s^{-1} Mpc^{-1} Uncertainty from the Hubble Space Telescope and the SH0ES Team*, *Astrophys. J. Lett.* **934** (2022) L7 [arXiv:2112.04510] [INSPIRE].

[6] DES collaboration, *Dark Energy Survey Year 3 results: Cosmology from cosmic shear and robustness to modeling uncertainty*, *Phys. Rev. D* **105** (2022) 023515 [arXiv:2105.13544] [INSPIRE].

[9] For Gaussian statistics (i.e. a normal probability distribution) the desired CL is related to S by

$$\mathrm{CL}(S) = \frac{1}{\sqrt{2\pi}} \int_{-\infty}^{S} e^{-t^2/2}\, dt.$$

JCAP05(2024)097

[7] DES collaboration, *Dark Energy Survey Year 3 results: Constraints on extensions to ΛCDM with weak lensing and galaxy clustering*, *Phys. Rev. D* **107** (2023) 083504 [arXiv:2207.05766] [INSPIRE].

[8] C. Heymans et al., *KiDS-1000 Cosmology: Multi-probe weak gravitational lensing and spectroscopic galaxy clustering constraints*, *Astron. Astrophys.* **646** (2021) A140 [arXiv:2007.15632] [INSPIRE].

[9] KiDS collaboration, *KiDS-1000 Cosmology: Constraints beyond flat ΛCDM*, *Astron. Astrophys.* **649** (2021) A88 [arXiv:2010.16416] [INSPIRE].

[10] E. Di Valentino et al., *Cosmology Intertwined III: $f\sigma_8$ and S_8*, *Astropart. Phys.* **131** (2021) 102604 [arXiv:2008.11285] [INSPIRE].

[11] Kilo-Degree Survey and Dark Energy Survey collaborations, *DES Y3 + KiDS-1000: Consistent cosmology combining cosmic shear surveys*, *Open J. Astrophys.* **6** (2023) 2305.17173 [arXiv:2305.17173] [INSPIRE].

[12] P. Santini et al., *Early Results from GLASS-JWST. XI. Stellar Masses and Mass-to-light Ratio of $z > 7$ Galaxies*, *Astrophys. J. Lett.* **942** (2023) L27 [arXiv:2207.11379].

[13] M. Castellano et al., *Early Results from GLASS-JWST. III. Galaxy Candidates at $z \sim 9$–15*, *Astrophys. J. Lett.* **938** (2022) L15 [arXiv:2207.09436].

[14] S.L. Finkelstein et al., *CEERS Key Paper. I. An Early Look into the First 500 Myr of Galaxy Formation with JWST*, *Astrophys. J. Lett.* **946** (2023) L13 [arXiv:2211.05792].

[15] R.P. Naidu et al., *Two Remarkably Luminous Galaxy Candidates at $z \approx 10$–12 Revealed by JWST*, *Astrophys. J. Lett.* **940** (2022) L14 [arXiv:2207.09434].

[16] T. Treu et al., *The GLASS-JWST Early Release Science Program. I. Survey Design and Release Plans*, *Astrophys. J.* **935** (2022) 110 [arXiv:2206.07978] [INSPIRE].

[17] Y. Harikane et al., *A Comprehensive Study of Galaxies at $z \sim 9$–16 Found in the Early JWST Data: Ultraviolet Luminosity Functions and Cosmic Star Formation History at the Pre-reionization Epoch*, *Astrophys. J. Suppl.* **265** (2023) 5 [arXiv:2208.01612] [INSPIRE].

[18] P.G. Pérez-González et al., *CEERS Key Paper. IV. A Triality in the Nature of HST-dark Galaxies*, *Astrophys. J. Lett.* **946** (2023) L16 [arXiv:2211.00045].

[19] C. Papovich et al., *CEERS Key Paper. V. Galaxies at $4 < z < 9$ Are Bluer than They Appear — Characterizing Galaxy Stellar Populations from Rest-frame $\sim 1\,\mu$m Imaging*, *Astrophys. J. Lett.* **949** (2023) L18 [arXiv:2301.00027].

[20] I. Labbé et al., *A population of red candidate massive galaxies ~ 600 Myr after the Big Bang*, *Nature* **616** (2023) 266 [arXiv:2207.12446] [INSPIRE].

[21] M. Boylan-Kolchin, *Stress testing ΛCDM with high-redshift galaxy candidates*, *Nature Astron.* **7** (2023) 731 [arXiv:2208.01611] [INSPIRE].

[22] Y.-Y. Wang, L. Lei, G.-W. Yuan and Y.-Z. Fan, *Modeling the JWST High-redshift Galaxies with a General Formation Scenario and the Consistency with the ΛCDM Model*, *Astrophys. J. Lett.* **954** (2023) L48 [arXiv:2307.12487] [INSPIRE].

[23] G. Sun et al., *Bursty Star Formation Naturally Explains the Abundance of Bright Galaxies at Cosmic Dawn*, *Astrophys. J. Lett.* **955** (2023) L35 [arXiv:2307.15305] [INSPIRE].

[24] P. Arrabal Haro et al., *Spectroscopic Confirmation of CEERS NIRCam-selected Galaxies at $z \simeq 8$–10*, *Astrophys. J. Lett.* **951** (2023) L22 [arXiv:2304.05378].

JCAP05(2024)097

[25] R. Bouwens et al., *UV luminosity density results at $z > 8$ from the first JWST/NIRCam fields: limitations of early data sets and the need for spectroscopy*, *Mon. Not. Roy. Astron. Soc.* **523** (2023) 1009 [arXiv:2212.06683] [INSPIRE].

[26] M. Xiao et al., *Massive Optically Dark Galaxies Unveiled by JWST Challenge Galaxy Formation Models*, arXiv:2309.02492.

[27] L. Vujeva et al., *Efficient survey design for finding high-redshift galaxies with JWST*, arXiv:2310.15284.

[28] C.C. Williams et al., *The galaxies missed by Hubble and ALMA: the contribution of extremely red galaxies to the cosmic census at $3 < z < 8$*, arXiv:2311.07483.

[29] R.K. Cochrane, D. Anglés-Alcázar, F. Cullen and C.C. Hayward, *Disappearing Galaxies: The Orientation Dependence of JWST-bright, HST-dark, Star-forming Galaxy Selection*, *Astrophys. J.* **961** (2024) 37 [arXiv:2310.08829].

[30] G. Desprez et al., *ΛCDM not dead yet: massive high-z Balmer break galaxies are less common than previously reported*, arXiv:2310.03063 [INSPIRE].

[31] Y. Qin, S. Balu and J.S.B. Wyithe, *Implications of $z \gtrsim 12$ JWST galaxies for galaxy formation at high redshift*, *Mon. Not. Roy. Astron. Soc.* **526** (2023) 1324 [arXiv:2305.17959] [INSPIRE].

[32] M. Forconi et al., *Do the early galaxies observed by JWST disagree with Planck's CMB polarization measurements?*, *JCAP* **10** (2023) 012 [arXiv:2306.07781] [INSPIRE].

[33] W. Giarè, E. Di Valentino and A. Melchiorri, *Measuring the reionization optical depth without large-scale CMB polarization*, *Phys. Rev. D* **109** (2024) 103519 [arXiv:2312.06482] [INSPIRE].

[34] S.A. Adil, U. Mukhopadhyay, A.A. Sen and S. Vagnozzi, *Dark energy in light of the early JWST observations: case for a negative cosmological constant?*, *JCAP* **10** (2023) 072 [arXiv:2307.12763] [INSPIRE].

[35] N. Menci et al., *High-redshift Galaxies from Early JWST Observations: Constraints on Dark Energy Models*, *Astrophys. J. Lett.* **938** (2022) L5 [arXiv:2208.11471] [INSPIRE].

[36] D. Wang and Y. Liu, *JWST high redshift galaxy observations have a strong tension with Planck CMB measurements*, arXiv:2301.00347 [INSPIRE].

[37] Y. Gong, B. Yue, Y. Cao and X. Chen, *Fuzzy Dark Matter as a Solution to Reconcile the Stellar Mass Density of High-z Massive Galaxies and Reionization History*, *Astrophys. J.* **947** (2023) 28 [arXiv:2209.13757] [INSPIRE].

[38] A. Zhitnitsky, *Structure formation paradigm and axion quark nugget dark matter model*, *Phys. Dark Univ.* **40** (2023) 101217 [arXiv:2302.00010] [INSPIRE].

[39] P. Dayal and S.K. Giri, *Warm dark matter constraints from the JWST*, *Mon. Not. Roy. Astron. Soc.* **528** (2024) 2784 [arXiv:2303.14239] [INSPIRE].

[40] U. Maio and M. Viel, *JWST high-redshift galaxy constraints on warm and cold dark matter models*, *Astron. Astrophys.* **672** (2023) A71 [arXiv:2211.03620] [INSPIRE].

[41] G. Domènech, D. Inman, A. Kusenko and M. Sasaki, *Halo formation from Yukawa forces in the very early Universe*, *Phys. Rev. D* **108** (2023) 103543 [arXiv:2304.13053] [INSPIRE].

[42] B. Liu and V. Bromm, *Accelerating Early Massive Galaxy Formation with Primordial Black Holes*, *Astrophys. J. Lett.* **937** (2022) L30 [arXiv:2208.13178] [INSPIRE].

[43] G.-W. Yuan et al., *Rapidly growing primordial black holes as seeds of the massive high-redshift JWST Galaxies*, arXiv:2303.09391 [INSPIRE].

JCAP05(2024)097

[44] G. Hütsi et al., *Did JWST observe imprints of axion miniclusters or primordial black holes?*, *Phys. Rev. D* **107** (2023) 043502 [arXiv:2211.02651] [INSPIRE].

[45] H. Jiao, R. Brandenberger and A. Refregier, *Early structure formation from cosmic string loops in light of early JWST observations*, *Phys. Rev. D* **108** (2023) 043510 [arXiv:2304.06429] [INSPIRE].

[46] M. Biagetti, G. Franciolini and A. Riotto, *High-redshift JWST Observations and Primordial Non-Gaussianity*, *Astrophys. J.* **944** (2023) 113 [arXiv:2210.04812] [INSPIRE].

[47] N. Menci et al., *Negative cosmological constant in the dark energy sector: tests from JWST photometric and spectroscopic observations of high-redshift galaxies*, arXiv:2401.12659 [INSPIRE].

[48] P. Parashari and R. Laha, *Primordial power spectrum in light of JWST observations of high redshift galaxies*, *Mon. Not. Roy. Astron. Soc.* **526** (2023) L63 [arXiv:2305.00999] [INSPIRE].

[49] C.C. Lovell et al., *Extreme value statistics of the halo and stellar mass distributions at high redshift: are JWST results in tension with ΛCDM?*, *Mon. Not. Roy. Astron. Soc.* **518** (2022) 2511 [arXiv:2208.10479] [INSPIRE].

[50] M. Haslbauer, P. Kroupa, A.H. Zonoozi and H. Haghi, *Has JWST Already Falsified Dark-matter-driven Galaxy Formation?*, *Astrophys. J. Lett.* **939** (2022) L31 [arXiv:2210.14915] [INSPIRE].

[51] G. Gandolfi, A. Lapi, T. Ronconi and L. Danese, *Astroparticle Constraints from the Cosmic Star Formation Rate Density at High Redshift: Current Status and Forecasts for JWST*, *Universe* **8** (2022) 589 [arXiv:2211.02840] [INSPIRE].

[52] N. Lovyagin, A. Raikov, V. Yershov and Y. Lovyagin, *Cosmological Model Tests with JWST*, *Galaxies* **10** (2022) 108 [arXiv:2212.06575] [INSPIRE].

[53] P. Wang et al., *Exploring the Dark Energy Equation of State with JWST*, arXiv:2307.11374 [INSPIRE].

[54] S. Hirano and N. Yoshida, *Early Structure Formation from Primordial Density Fluctuations with a Blue, Tilted Power Spectrum: High-redshift Galaxies*, *Astrophys. J.* **963** (2024) 2 [arXiv:2306.11993] [INSPIRE].

[55] E.A. Paraskevas and L. Perivolaropoulos, *The density of virialized clusters as a probe of dark energy*, arXiv:2308.07046 [INSPIRE].

[56] A. Pallottini and A. Ferrara, *Stochastic star formation in early galaxies: Implications for the James Webb Space Telescope*, *Astron. Astrophys.* **677** (2023) L4 [arXiv:2307.03219] [INSPIRE].

[57] A. Ferrara, A. Pallottini and P. Dayal, *On the stunning abundance of super-early, luminous galaxies revealed by JWST*, *Mon. Not. Roy. Astron. Soc.* **522** (2023) 3986 [arXiv:2208.00720] [INSPIRE].

[58] F. Pacucci et al., *JWST CEERS and JADES Active Galaxies at $z = 4$–7 Violate the Local $M_\bullet$–$M_\star$ Relation at $> 3\sigma$: Implications for Low-mass Black Holes and Seeding Models*, *Astrophys. J. Lett.* **957** (2023) L3 [arXiv:2308.12331] [INSPIRE].

[59] H. Mo, Y. Chen and H. Wang, *A two-phase model of galaxy formation: I. The growth of galaxies and supermassive black holes*, arXiv:2311.05030 [INSPIRE].

[60] U. Maio et al., *Early structure formation in quintessence models and its implications for cosmic reionisation from first stars*, *Mon. Not. Roy. Astron. Soc.* **373** (2006) 869 [astro-ph/0607409] [INSPIRE].

[61] M. Baldi, V. Pettorino, G. Robbers and V. Springel, *Hydrodynamical N-body simulations of coupled dark energy cosmologies*, *Mon. Not. Roy. Astron. Soc.* **403** (2010) 1684 [arXiv:0812.3901] [INSPIRE].

[62] M. Baldi, *Dark Energy Simulations*, *Phys. Dark Univ.* **1** (2012) 162 [arXiv:1210.6650] [INSPIRE].

[63] A. Barreira, B. Li, C.M. Baugh and S. Pascoli, *Spherical collapse in Galileon gravity: fifth force solutions, halo mass function and halo bias*, *JCAP* **11** (2013) 056 [arXiv:1308.3699] [INSPIRE].

[64] U. Maio and M. Viel, *The First Billion Years of a Warm Dark Matter Universe*, *Mon. Not. Roy. Astron. Soc.* **446** (2015) 2760 [arXiv:1409.6718] [INSPIRE].

[65] J. Adamek, R. Durrer and M. Kunz, *Relativistic N-body simulations with massive neutrinos*, *JCAP* **11** (2017) 004 [arXiv:1707.06938] [INSPIRE].

[66] G. Risaliti and E. Lusso, *Cosmological constraints from the Hubble diagram of quasars at high redshifts*, *Nature Astron.* **3** (2019) 272 [arXiv:1811.02590] [INSPIRE].

[67] T. Yang, A. Banerjee and E.Ó. Colgáin, *Cosmography and flat ΛCDM tensions at high redshift*, *Phys. Rev. D* **102** (2020) 123532 [arXiv:1911.01681] [INSPIRE].

[68] C. Wetterich, *Phenomenological parameterization of quintessence*, *Phys. Lett. B* **594** (2004) 17 [astro-ph/0403289] [INSPIRE].

[69] M. Doran and G. Robbers, *Early dark energy cosmologies*, *JCAP* **06** (2006) 026 [astro-ph/0601544] [INSPIRE].

[70] L. Hollenstein, D. Sapone, R. Crittenden and B.M. Schaefer, *Constraints on early dark energy from CMB lensing and weak lensing tomography*, *JCAP* **04** (2009) 012 [arXiv:0902.1494] [INSPIRE].

[71] E. Calabrese et al., *Future CMB Constraints on Early, Cold, or Stressed Dark Energy*, *Phys. Rev. D* **83** (2011) 023011 [arXiv:1010.5612] [INSPIRE].

[72] E. Calabrese et al., *Limits on Dark Radiation, Early Dark Energy, and Relativistic Degrees of Freedom*, *Phys. Rev. D* **83** (2011) 123504 [arXiv:1103.4132] [INSPIRE].

[73] V. Pettorino, L. Amendola and C. Wetterich, *How early is early dark energy?*, *Phys. Rev. D* **87** (2013) 083009 [arXiv:1301.5279] [INSPIRE].

[74] M. Archidiacono, L. Lopez-Honorez and O. Mena, *Current constraints on early and stressed dark energy models and future 21 cm perspectives*, *Phys. Rev. D* **90** (2014) 123016 [arXiv:1409.1802] [INSPIRE].

[75] V. Poulin, T.L. Smith and T. Karwal, *The Ups and Downs of Early Dark Energy solutions to the Hubble tension: A review of models, hints and constraints circa 2023*, *Phys. Dark Univ.* **42** (2023) 101348 [arXiv:2302.09032] [INSPIRE].

[76] V. Poulin et al., *Cosmological implications of ultralight axionlike fields*, *Phys. Rev. D* **98** (2018) 083525 [arXiv:1806.10608] [INSPIRE].

[77] V. Poulin, K.K. Boddy, S. Bird and M. Kamionkowski, *Implications of an extended dark energy cosmology with massive neutrinos for cosmological tensions*, *Phys. Rev. D* **97** (2018) 123504 [arXiv:1803.02474] [INSPIRE].

[78] T.L. Smith, V. Poulin and M.A. Amin, *Oscillating scalar fields and the Hubble tension: a resolution with novel signatures*, *Phys. Rev. D* **101** (2020) 063523 [arXiv:1908.06995] [INSPIRE].

[79] F. Niedermann and M.S. Sloth, *New early dark energy*, *Phys. Rev. D* **103** (2021) L041303 [arXiv:1910.10739] [INSPIRE].

JCAP05(2024)097

[80] F. Niedermann and M.S. Sloth, *Resolving the Hubble tension with new early dark energy*, *Phys. Rev. D* **102** (2020) 063527 [arXiv:2006.06686] [INSPIRE].

[81] R. Murgia, G.F. Abellán and V. Poulin, *Early dark energy resolution to the Hubble tension in light of weak lensing surveys and lensing anomalies*, *Phys. Rev. D* **103** (2021) 063502 [arXiv:2009.10733] [INSPIRE].

[82] G. Ye and Y.-S. Piao, *Is the Hubble tension a hint of AdS phase around recombination?*, *Phys. Rev. D* **101** (2020) 083507 [arXiv:2001.02451] [INSPIRE].

[83] A. Klypin et al., *Clustering and Halo Abundances in Early Dark Energy Cosmological Models*, *Mon. Not. Roy. Astron. Soc.* **504** (2021) 769 [arXiv:2006.14910] [INSPIRE].

[84] J.C. Hill, E. McDonough, M.W. Toomey and S. Alexander, *Early dark energy does not restore cosmological concordance*, *Phys. Rev. D* **102** (2020) 043507 [arXiv:2003.07355] [INSPIRE].

[85] L. Herold, E.G.M. Ferreira and E. Komatsu, *New Constraint on Early Dark Energy from Planck and BOSS Data Using the Profile Likelihood*, *Astrophys. J. Lett.* **929** (2022) L16 [arXiv:2112.12140] [INSPIRE].

[86] L. Herold and E.G.M. Ferreira, *Resolving the Hubble tension with early dark energy*, *Phys. Rev. D* **108** (2023) 043513 [arXiv:2210.16296] [INSPIRE].

[87] A. Reeves et al., *Restoring cosmological concordance with early dark energy and massive neutrinos?*, *Mon. Not. Roy. Astron. Soc.* **520** (2023) 3688 [arXiv:2207.01501] [INSPIRE].

[88] J.-Q. Jiang and Y.-S. Piao, *Toward early dark energy and ns=1 with Planck, ACT, and SPT observations*, *Phys. Rev. D* **105** (2022) 103514 [arXiv:2202.13379] [INSPIRE].

[89] T. Simon, P. Zhang, V. Poulin and T.L. Smith, *Updated constraints from the effective field theory analysis of the BOSS power spectrum on early dark energy*, *Phys. Rev. D* **107** (2023) 063505 [arXiv:2208.05930] [INSPIRE].

[90] T.L. Smith et al., *Hints of early dark energy in Planck, SPT, and ACT data: New physics or systematics?*, *Phys. Rev. D* **106** (2022) 043526 [arXiv:2202.09379] [INSPIRE].

[91] M. Kamionkowski and A.G. Riess, *The Hubble Tension and Early Dark Energy*, *Ann. Rev. Nucl. Part. Sci.* **73** (2023) 153 [arXiv:2211.04492] [INSPIRE].

[92] F. Niedermann and M.S. Sloth, *New Early Dark Energy as a solution to the H_0 and S_8 tensions*, arXiv:2307.03481 [INSPIRE].

[93] J.S. Cruz, F. Niedermann and M.S. Sloth, *Cold New Early Dark Energy pulls the trigger on the H_0 and S_8 tensions: a simultaneous solution to both tensions without new ingredients*, *JCAP* **11** (2023) 033 [arXiv:2305.08895] [INSPIRE].

[94] J.R. Eskilt et al., *Constraints on Early Dark Energy from Isotropic Cosmic Birefringence*, *Phys. Rev. Lett.* **131** (2023) 121001 [arXiv:2303.15369] [INSPIRE].

[95] T.L. Smith and V. Poulin, *Current small-scale CMB constraints to axionlike early dark energy*, *Phys. Rev. D* **109** (2024) 103506 [arXiv:2309.03265] [INSPIRE].

[96] R.K. Sharma, S. Das and V. Poulin, *Early dark energy beyond slow-roll: Implications for cosmic tensions*, *Phys. Rev. D* **109** (2024) 043530 [arXiv:2309.00401] [INSPIRE].

[97] G. Efstathiou, E. Rosenberg and V. Poulin, *Improved Planck constraints on axion-like early dark energy as a resolution of the Hubble tension*, arXiv:2311.00524 [INSPIRE].

[98] R. Gsponer et al., *Cosmological constraints on early dark energy from the full shape analysis of eBOSS DR16*, *Mon. Not. Roy. Astron. Soc.* **530** (2024) 3075 [arXiv:2312.01977] [INSPIRE].

JCAP05(2024)097

[99] S. Goldstein, J.C. Hill, V. Iršič and B.D. Sherwin, *Canonical Hubble-Tension-Resolving Early Dark Energy Cosmologies Are Inconsistent with the Lyman-α Forest*, *Phys. Rev. Lett.* **131** (2023) 201001 [arXiv:2303.00746] [INSPIRE].

[100] E. Abdalla et al., *Cosmology intertwined: A review of the particle physics, astrophysics, and cosmology associated with the cosmological tensions and anomalies*, *JHEAp* **34** (2022) 49 [arXiv:2203.06142] [INSPIRE].

[101] J. Valiviita, E. Majerotto and R. Maartens, *Instability in interacting dark energy and dark matter fluids*, *JCAP* **07** (2008) 020 [arXiv:0804.0232] [INSPIRE].

[102] M.B. Gavela et al., *Dark coupling*, *JCAP* **07** (2009) 034 [*Erratum ibid.* **05** (2010) E01] [arXiv:0901.1611] [INSPIRE].

[103] V. Salvatelli et al., *Indications of a late-time interaction in the dark sector*, *Phys. Rev. Lett.* **113** (2014) 181301 [arXiv:1406.7297] [INSPIRE].

[104] J. Solà, A. Gómez-Valent and J. de Cruz Pérez, *First evidence of running cosmic vacuum: challenging the concordance model*, *Astrophys. J.* **836** (2017) 43 [arXiv:1602.02103] [INSPIRE].

[105] E. Di Valentino, A. Melchiorri and O. Mena, *Can interacting dark energy solve the H_0 tension?*, *Phys. Rev. D* **96** (2017) 043503 [arXiv:1704.08342] [INSPIRE].

[106] S. Kumar and R.C. Nunes, *Echo of interactions in the dark sector*, *Phys. Rev. D* **96** (2017) 103511 [arXiv:1702.02143] [INSPIRE].

[107] B. Wang, E. Abdalla, F. Atrio-Barandela and D. Pavon, *Dark Matter and Dark Energy Interactions: Theoretical Challenges, Cosmological Implications and Observational Signatures*, *Rept. Prog. Phys.* **79** (2016) 096901 [arXiv:1603.08299] [INSPIRE].

[108] J. Solà Peracaula, J. de Cruz Pérez and A. Gómez-Valent, *Possible signals of vacuum dynamics in the Universe*, *Mon. Not. Roy. Astron. Soc.* **478** (2018) 4357 [arXiv:1703.08218] [INSPIRE].

[109] J. Solà, A. Gómez-Valent and J. de Cruz Pérez, *The H_0 tension in light of vacuum dynamics in the Universe*, *Phys. Lett. B* **774** (2017) 317 [arXiv:1705.06723] [INSPIRE].

[110] A. Gómez-Valent and J. Solà Peracaula, *Density perturbations for running vacuum: a successful approach to structure formation and to the σ_8-tension*, *Mon. Not. Roy. Astron. Soc.* **478** (2018) 126 [arXiv:1801.08501] [INSPIRE].

[111] M. Martinelli et al., *Constraints on the interacting vacuum-geodesic CDM scenario*, *Mon. Not. Roy. Astron. Soc.* **488** (2019) 3423 [arXiv:1902.10694] [INSPIRE].

[112] W. Yang, S. Pan, R.C. Nunes and D.F. Mota, *Dark calling Dark: Interaction in the dark sector in presence of neutrino properties after Planck CMB final release*, *JCAP* **04** (2020) 008 [arXiv:1910.08821] [INSPIRE].

[113] E. Di Valentino, A. Melchiorri, O. Mena and S. Vagnozzi, *Interacting dark energy in the early 2020s: A promising solution to the H_0 and cosmic shear tensions*, *Phys. Dark Univ.* **30** (2020) 100666 [arXiv:1908.04281] [INSPIRE].

[114] S. Pan, W. Yang, C. Singha and E.N. Saridakis, *Observational constraints on sign-changeable interaction models and alleviation of the H_0 tension*, *Phys. Rev. D* **100** (2019) 083539 [arXiv:1903.10969] [INSPIRE].

[115] S. Kumar, R.C. Nunes and S.K. Yadav, *Dark sector interaction: a remedy of the tensions between CMB and LSS data*, *Eur. Phys. J. C* **79** (2019) 576 [arXiv:1903.04865] [INSPIRE].

[116] W. Yang et al., *Tale of stable interacting dark energy, observational signatures, and the H_0 tension*, *JCAP* **09** (2018) 019 [arXiv:1805.08252] [INSPIRE].

JCAP05(2024)097

[117] M. Escudero et al., *Exploring dark matter microphysics with galaxy surveys*, *JCAP* **09** (2015) 034 [arXiv:1505.06735] [INSPIRE].

[118] S. Kumar and R.C. Nunes, *Probing the interaction between dark matter and dark energy in the presence of massive neutrinos*, *Phys. Rev. D* **94** (2016) 123511 [arXiv:1608.02454] [INSPIRE].

[119] R. Murgia, S. Gariazzo and N. Fornengo, *Constraints on the Coupling between Dark Energy and Dark Matter from CMB data*, *JCAP* **04** (2016) 014 [arXiv:1602.01765] [INSPIRE].

[120] A. Pourtsidou and T. Tram, *Reconciling CMB and structure growth measurements with dark energy interactions*, *Phys. Rev. D* **94** (2016) 043518 [arXiv:1604.04222] [INSPIRE].

[121] W. Yang, S. Pan, L. Xu and D.F. Mota, *Effects of anisotropic stress in interacting dark matter-dark energy scenarios*, *Mon. Not. Roy. Astron. Soc.* **482** (2019) 1858 [arXiv:1804.08455] [INSPIRE].

[122] B.J. Barros, L. Amendola, T. Barreiro and N.J. Nunes, *Coupled quintessence with a ΛCDM background: removing the σ_8 tension*, *JCAP* **01** (2019) 007 [arXiv:1802.09216] [INSPIRE].

[123] W. Yang, O. Mena, S. Pan and E. Di Valentino, *Dark sectors with dynamical coupling*, *Phys. Rev. D* **100** (2019) 083509 [arXiv:1906.11697] [INSPIRE].

[124] S. Pan et al., *Interacting scenarios with dynamical dark energy: Observational constraints and alleviation of the H_0 tension*, *Phys. Rev. D* **100** (2019) 103520 [arXiv:1907.07540] [INSPIRE].

[125] E. Di Valentino, A. Melchiorri, O. Mena and S. Vagnozzi, *Nonminimal dark sector physics and cosmological tensions*, *Phys. Rev. D* **101** (2020) 063502 [arXiv:1910.09853] [INSPIRE].

[126] E. Di Valentino and O. Mena, *A fake Interacting Dark Energy detection?*, *Mon. Not. Roy. Astron. Soc.* **500** (2020) L22 [arXiv:2009.12620] [INSPIRE].

[127] Y. Yao and X.-H. Meng, *Relieve the H_0 tension with a new coupled generalized three-form dark energy model*, *Phys. Dark Univ.* **33** (2021) 100852 [arXiv:2011.09160] [INSPIRE].

[128] M. Lucca and D.C. Hooper, *Shedding light on dark matter-dark energy interactions*, *Phys. Rev. D* **102** (2020) 123502 [arXiv:2002.06127] [INSPIRE].

[129] E. Di Valentino et al., *Interacting Dark Energy in a closed universe*, *Mon. Not. Roy. Astron. Soc.* **502** (2021) L23 [arXiv:2011.00283] [INSPIRE].

[130] A. Gómez-Valent, V. Pettorino and L. Amendola, *Update on coupled dark energy and the H_0 tension*, *Phys. Rev. D* **101** (2020) 123513 [arXiv:2004.00610] [INSPIRE].

[131] W. Yang et al., *All-inclusive interacting dark sector cosmologies*, *Phys. Rev. D* **101** (2020) 083509 [arXiv:2001.10852] [INSPIRE].

[132] Y.-H. Yao and X.-H. Meng, *A new coupled three-form dark energy model and implications for the H_0 tension*, *Phys. Dark Univ.* **30** (2020) 100729 [arXiv:2205.14928] [INSPIRE].

[133] S. Pan, W. Yang and A. Paliathanasis, *Non-linear interacting cosmological models after Planck 2018 legacy release and the H_0 tension*, *Mon. Not. Roy. Astron. Soc.* **493** (2020) 3114 [arXiv:2002.03408] [INSPIRE].

[134] E. Di Valentino, *A combined analysis of the H_0 late time direct measurements and the impact on the Dark Energy sector*, *Mon. Not. Roy. Astron. Soc.* **502** (2021) 2065 [arXiv:2011.00246] [INSPIRE].

[135] N.B. Hogg et al., *Latest evidence for a late time vacuum-geodesic CDM interaction*, *Phys. Dark Univ.* **29** (2020) 100583 [arXiv:2002.10449] [INSPIRE].

[136] J. Solà Peracaula, A. Gómez-Valent, J. de Cruz Pérez and C. Moreno-Pulido, *Running vacuum against the H_0 and σ_8 tensions*, *EPL* **134** (2021) 19001 [arXiv:2102.12758] [INSPIRE].

JCAP05(2024)097

[137] M. Lucca, *Dark energy-dark matter interactions as a solution to the S8 tension*, *Phys. Dark Univ.* **34** (2021) 100899 [arXiv:2105.09249] [INSPIRE].

[138] S. Kumar, *Remedy of some cosmological tensions via effective phantom-like behavior of interacting vacuum energy*, *Phys. Dark Univ.* **33** (2021) 100862 [arXiv:2102.12902] [INSPIRE].

[139] W. Yang et al., *2021-H0 odyssey: closed, phantom and interacting dark energy cosmologies*, *JCAP* **10** (2021) 008 [arXiv:2101.03129] [INSPIRE].

[140] L.-Y. Gao, Z.-W. Zhao, S.-S. Xue and X. Zhang, *Relieving the H 0 tension with a new interacting dark energy model*, *JCAP* **07** (2021) 005 [arXiv:2101.10714] [INSPIRE].

[141] W. Yang, S. Pan, L. Aresté Saló and J. de Haro, *Theoretical and observational bounds on some interacting vacuum energy scenarios*, *Phys. Rev. D* **103** (2021) 083520 [arXiv:2104.04505] [INSPIRE].

[142] M. Lucca, *Multi-interacting dark energy and its cosmological implications*, *Phys. Rev. D* **104** (2021) 083510 [arXiv:2106.15196] [INSPIRE].

[143] A. Halder and M. Pandey, *Probing the effects of primordial black holes on 21-cm EDGES signal along with interacting dark energy and dark matter-baryon scattering*, *Mon. Not. Roy. Astron. Soc.* **508** (2021) 3446 [arXiv:2101.05228] [INSPIRE].

[144] K. Kaneta, H.-S. Lee, J. Lee and J. Yi, *Gauged quintessence*, *JCAP* **02** (2023) 005 [arXiv:2208.09229] [INSPIRE].

[145] S. Gariazzo, E. Di Valentino, O. Mena and R.C. Nunes, *Late-time interacting cosmologies and the Hubble constant tension*, *Phys. Rev. D* **106** (2022) 023530 [arXiv:2111.03152] [INSPIRE].

[146] R.C. Nunes and E. Di Valentino, *Dark sector interaction and the supernova absolute magnitude tension*, *Phys. Rev. D* **104** (2021) 063529 [arXiv:2107.09151] [INSPIRE].

[147] W. Yang, S. Pan, O. Mena and E. Di Valentino, *On the dynamics of a dark sector coupling*, *JHEAp* **40** (2023) 19 [arXiv:2209.14816] [INSPIRE].

[148] R.C. Nunes et al., *New tests of dark sector interactions from the full-shape galaxy power spectrum*, *Phys. Rev. D* **105** (2022) 123506 [arXiv:2203.08093] [INSPIRE].

[149] L.W.K. Goh, A. Gómez-Valent, V. Pettorino and M. Kilbinger, *Constraining constant and tomographic coupled dark energy with low-redshift and high-redshift probes*, *Phys. Rev. D* **107** (2023) 083503 [arXiv:2211.13588] [INSPIRE].

[150] A. Gómez-Valent et al., *Coupled and uncoupled early dark energy, massive neutrinos, and the cosmological tensions*, *Phys. Rev. D* **106** (2022) 103522 [arXiv:2207.14487] [INSPIRE].

[151] M.A. van der Westhuizen and A. Abebe, *Interacting dark energy: clarifying the cosmological implications and viability conditions*, *JCAP* **01** (2024) 048 [arXiv:2302.11949] [INSPIRE].

[152] Y. Zhai et al., *A consistent view of interacting dark energy from multiple CMB probes*, *JCAP* **07** (2023) 032 [arXiv:2303.08201] [INSPIRE].

[153] A. Bernui et al., *Exploring the H0 tension and the evidence for dark sector interactions from 2D BAO measurements*, *Phys. Rev. D* **107** (2023) 103531 [arXiv:2301.06097] [INSPIRE].

[154] J. de Cruz Pérez and J. Solà Peracaula, *Running vacuum in Brans & Dicke theory: A possible cure for the σ_8 and H_0 tensions*, *Phys. Dark Univ.* **43** (2024) 101406 [arXiv:2302.04807] [INSPIRE].

[155] L.A. Escamilla, O. Akarsu, E. Di Valentino and J.A. Vazquez, *Model-independent reconstruction of the interacting dark energy kernel: Binned and Gaussian process*, *JCAP* **11** (2023) 051 [arXiv:2305.16290] [INSPIRE].

JCAP05(2024)097

[156] J.-H. He, B. Wang and E. Abdalla, *Stability of the curvature perturbation in dark sectors' mutual interacting models*, *Phys. Lett. B* **671** (2009) 139 [arXiv:0807.3471] [INSPIRE].

[157] M.B. Gavela, L. Lopez Honorez, O. Mena and S. Rigolin, *Dark Coupling and Gauge Invariance*, *JCAP* **11** (2010) 044 [arXiv:1005.0295] [INSPIRE].

[158] L. Lopez Honorez et al., *Coupled dark matter-dark energy in light of near Universe observations*, *JCAP* **09** (2010) 029 [arXiv:1006.0877] [INSPIRE].

[159] B.M. Jackson, A. Taylor and A. Berera, *On the large-scale instability in interacting dark energy and dark matter fluids*, *Phys. Rev. D* **79** (2009) 043526 [arXiv:0901.3272] [INSPIRE].

[160] T. Clemson et al., *Interacting Dark Energy — constraints and degeneracies*, *Phys. Rev. D* **85** (2012) 043007 [arXiv:1109.6234] [INSPIRE].

[161] Y.-H. Li, J.-F. Zhang and X. Zhang, *Parametrized Post-Friedmann Framework for Interacting Dark Energy*, *Phys. Rev. D* **90** (2014) 063005 [arXiv:1404.5220] [INSPIRE].

[162] Y.-H. Li, J.-F. Zhang and X. Zhang, *Exploring the full parameter space for an interacting dark energy model with recent observations including redshift-space distortions: Application of the parametrized post-Friedmann approach*, *Phys. Rev. D* **90** (2014) 123007 [arXiv:1409.7205] [INSPIRE].

[163] R.-Y. Guo, Y.-H. Li, J.-F. Zhang and X. Zhang, *Weighing neutrinos in the scenario of vacuum energy interacting with cold dark matter: application of the parameterized post-Friedmann approach*, *JCAP* **05** (2017) 040 [arXiv:1702.04189] [INSPIRE].

[164] X. Zhang, *Probing the interaction between dark energy and dark matter with the parametrized post-Friedmann approach*, *Sci. China Phys. Mech. Astron.* **60** (2017) 050431 [arXiv:1702.04564] [INSPIRE].

[165] R.-Y. Guo, J.-F. Zhang and X. Zhang, *Exploring neutrino mass and mass hierarchy in the scenario of vacuum energy interacting with cold dark matte*, *Chin. Phys. C* **42** (2018) 095103 [arXiv:1803.06910] [INSPIRE].

[166] J.-P. Dai and J. Xia, *Revisiting the Instability Problem of the Interacting Dark Energy Model in the Parameterized Post-Friedmann Framework*, *Astrophys. J.* **876** (2019) 125 [arXiv:1904.04149] [INSPIRE].

[167] S. Pan, G.S. Sharov and W. Yang, *Field theoretic interpretations of interacting dark energy scenarios and recent observations*, *Phys. Rev. D* **101** (2020) 103533 [arXiv:2001.03120] [INSPIRE].

[168] S. Tacchella et al., *A Redshift-independent Efficiency Model: Star Formation and Stellar Masses in Dark Matter Halos at $z \gtrsim 4$*, *Astrophys. J.* **868** (2018) 92 [arXiv:1806.03299] [INSPIRE].

[169] K. Chworowsky et al., *Evidence for a Shallow Evolution in the Volume Densities of Massive Galaxies at $z = 4$ to 8 from CEERS*, arXiv:2311.14804.

[170] S.W. Allen et al., *Constraints on dark energy from Chandra observations of the largest relaxed galaxy clusters*, *Mon. Not. Roy. Astron. Soc.* **353** (2004) 457 [astro-ph/0405340] [INSPIRE].

[171] A. Vikhlinin et al., *Chandra sample of nearby relaxed galaxy clusters: Mass, gas fraction, and mass-temperature relation*, *Astrophys. J.* **640** (2006) 691 [astro-ph/0507092] [INSPIRE].

[172] A.V. Kravtsov, D. Nagai and A.A. Vikhlinin, *Effects of cooling and star formation on the baryon fractions in clusters*, *Astrophys. J.* **625** (2005) 588 [astro-ph/0501227] [INSPIRE].

[173] S. Borgani and A. Kravtsov, *Cosmological simulations of galaxy clusters*, *Adv. Sci. Lett.* **4** (2011) 204 [arXiv:0906.4370] [INSPIRE].

JCAP05(2024)097

[174] A.B. Mantz et al., *Cosmology and astrophysics from relaxed galaxy clusters — II. Cosmological constraints*, *Mon. Not. Roy. Astron. Soc.* **440** (2014) 2077 [arXiv:1402.6212] [INSPIRE].

[175] K. Panchal and S. Desai, *Comparison of ΛCDM and $R_h = ct$ with updated galaxy cluster f_{gas} measurements using Bayesian inference*, arXiv:2401.11138 [INSPIRE].

[176] R.K. Sheth and G. Tormen, *Large scale bias and the peak background split*, *Mon. Not. Roy. Astron. Soc.* **308** (1999) 119 [astro-ph/9901122] [INSPIRE].

[177] R.K. Sheth, H.J. Mo and G. Tormen, *Ellipsoidal collapse and an improved model for the number and spatial distribution of dark matter haloes*, *Mon. Not. Roy. Astron. Soc.* **323** (2001) 1 [astro-ph/9907024] [INSPIRE].

[178] M. Maggiore and A. Riotto, *The Halo mass function from excursion set theory. II. The diffusing barrier*, *Astrophys. J.* **717** (2010) 515 [arXiv:0903.1250] [INSPIRE].

[179] I.E. Achitouv and P.S. Corasaniti, *Primordial Bispectrum and Trispectrum Contributions to the Non-Gaussian Excursion Set Halo Mass Function with Diffusive Drifting Barrier*, *Phys. Rev. D* **86** (2012) 083011 [arXiv:1207.4796] [INSPIRE].

[180] G. Despali et al., *The universality of the virial halo mass function and models for non-universality of other halo definitions*, *Mon. Not. Roy. Astron. Soc.* **456** (2016) 2486 [arXiv:1507.05627] [INSPIRE].

[181] R.J. Bouwens et al., *Evolution of the UV LF from $z \sim 15$ to $z \sim 8$ using new JWST NIRCam medium-band observations over the HUDF/XDF*, *Mon. Not. Roy. Astron. Soc.* **523** (2023) 1036.

[182] R. Navarro-Carrera et al., *Constraints on the Faint End of the Galaxy Stellar Mass Function at $z \simeq 4$–8 from Deep JWST Data*, *Astrophys. J.* **961** (2024) 207 [arXiv:2305.16141] [INSPIRE].

[183] J. Torrado and A. Lewis, *Cobaya: Code for Bayesian Analysis of hierarchical physical models*, *JCAP* **05** (2021) 057 [arXiv:2005.05290] [INSPIRE].

[184] J. Lesgourgues, *The Cosmic Linear Anisotropy Solving System (CLASS) I: Overview*, arXiv:1104.2932 [INSPIRE].

[185] D. Blas, J. Lesgourgues and T. Tram, *The Cosmic Linear Anisotropy Solving System (CLASS) II: Approximation schemes*, *JCAP* **07** (2011) 034 [arXiv:1104.2933] [INSPIRE].

[186] A. Lewis and S. Bridle, *Cosmological parameters from CMB and other data: A Monte Carlo approach*, *Phys. Rev. D* **66** (2002) 103511 [astro-ph/0205436] [INSPIRE].

[187] A. Lewis, *Efficient sampling of fast and slow cosmological parameters*, *Phys. Rev. D* **87** (2013) 103529 [arXiv:1304.4473] [INSPIRE].

[188] R.M. Neal, *Taking Bigger Metropolis Steps by Dragging Fast Variables*, math/0502099 [INSPIRE].

[189] Planck collaboration, *Planck 2018 results. V. CMB power spectra and likelihoods*, *Astron. Astrophys.* **641** (2020) A5 [arXiv:1907.12875] [INSPIRE].

[190] Planck collaboration, *Planck 2018 results. VIII. Gravitational lensing*, *Astron. Astrophys.* **641** (2020) A8 [arXiv:1807.06210] [INSPIRE].

[191] A. Gelman and D.B. Rubin, *Inference from Iterative Simulation Using Multiple Sequences*, *Statist. Sci.* **7** (1992) 457 [INSPIRE].

[192] E. Di Valentino, A. Melchiorri, Y. Fantaye and A. Heavens, *Bayesian evidence against the Harrison-Zel'dovich spectrum in tensions with cosmological data sets*, *Phys. Rev. D* **98** (2018) 063508 [arXiv:1808.09201] [INSPIRE].

JCAP05(2024)097

[193] G. Ye, B. Hu and Y.-S. Piao, *Implication of the Hubble tension for the primordial Universe in light of recent cosmological data*, *Phys. Rev. D* **104** (2021) 063510 [arXiv:2103.09729] [INSPIRE].

[194] G. Ye, J.-Q. Jiang and Y.-S. Piao, *Toward inflation with ns=1 in light of the Hubble tension and implications for primordial gravitational waves*, *Phys. Rev. D* **106** (2022) 103528 [arXiv:2205.02478] [INSPIRE].

[195] J.-Q. Jiang, G. Ye and Y.-S. Piao, *Return of Harrison-Zeldovich spectrum in light of recent cosmological tensions*, *Mon. Not. Roy. Astron. Soc.* **527** (2023) L54 [arXiv:2210.06125] [INSPIRE].

[196] F. Takahashi and W. Yin, *Cosmological implications of $n_s \approx 1$ in light of the Hubble tension*, *Phys. Lett. B* **830** (2022) 137143 [arXiv:2112.06710] [INSPIRE].

[197] J.-Q. Jiang, G. Ye and Y.-S. Piao, *Impact of the Hubble tension on the r-n_s contour*, *Phys. Lett. B* **851** (2024) 138588 [arXiv:2303.12345] [INSPIRE].

[198] Z.-Y. Peng and Y.-S. Piao, *Testing the ns-H0 scaling relation with Planck-independent CMB data*, *Phys. Rev. D* **109** (2024) 023519 [arXiv:2308.01012] [INSPIRE].

[199] M. Forconi, W. Giarè, E. Di Valentino and A. Melchiorri, *Cosmological constraints on slow roll inflation: An update*, *Phys. Rev. D* **104** (2021) 103528 [arXiv:2110.01695] [INSPIRE].

[200] ACT collaboration, *The Atacama Cosmology Telescope: DR4 Maps and Cosmological Parameters*, *JCAP* **12** (2020) 047 [arXiv:2007.07288] [INSPIRE].

[201] W. Handley and P. Lemos, *Quantifying the global parameter tensions between ACT, SPT and Planck*, *Phys. Rev. D* **103** (2021) 063529 [arXiv:2007.08496] [INSPIRE].

[202] E. Di Valentino, W. Giarè, A. Melchiorri and J. Silk, *Quantifying the global 'CMB tension' between the Atacama Cosmology Telescope and the Planck satellite in extended models of cosmology*, *Mon. Not. Roy. Astron. Soc.* **520** (2023) 210 [arXiv:2209.14054] [INSPIRE].

[203] W. Giarè et al., *Is the Harrison-Zel'dovich spectrum coming back? ACT preference for $n_s \sim 1$ and its discordance with Planck*, *Mon. Not. Roy. Astron. Soc.* **521** (2023) 2911 [arXiv:2210.09018] [INSPIRE].

[204] W. Giarè et al., *Inflationary potential as seen from different angles: model compatibility from multiple CMB missions*, *JCAP* **09** (2023) 019 [arXiv:2305.15378] [INSPIRE].

[205] E. Di Valentino, W. Giarè, A. Melchiorri and J. Silk, *Health checkup test of the standard cosmological model in view of recent cosmic microwave background anisotropies experiments*, *Phys. Rev. D* **106** (2022) 103506 [arXiv:2209.12872] [INSPIRE].

[206] R. Calderón, A. Shafieloo, D.K. Hazra and W. Sohn, *On the consistency of ΛCDM with CMB measurements in light of the latest Planck, ACT and SPT data*, *JCAP* **08** (2023) 059 [arXiv:2302.14300] [INSPIRE].

[207] W. Giarè, *CMB Anomalies and the Hubble Tension*, arXiv:2305.16919 [INSPIRE].

[208] W. Yang et al., *Dynamical dark energy after Planck CMB final release and H_0 tension*, *Mon. Not. Roy. Astron. Soc.* **501** (2021) 5845 [arXiv:2101.02168] [INSPIRE].

[209] L.A. Escamilla et al., *The state of the dark energy equation of state circa 2023*, arXiv:2307.14802 [INSPIRE].

[210] N. Gehrels, *Confidence limits for small numbers of events in astrophysical data*, *Astrophys. J.* **303** (1986) 336 [INSPIRE].

[211] H. Ebeling, *Improved approximations of poissonian errors for high confidence levels*, *Mon. Not. Roy. Astron. Soc.* **349** (2004) 768 [astro-ph/0301285] [INSPIRE].

JCAP05(2024)097